CREB REGULATES FOXP3^{+}ST-2^{+} T_{REGS} WITH ENHANCED IL-10 PRODUCTION

Sudheendra Hebbar Subramanyam[1], Judit Hriczko[1], Saskia Schulz[1], Thomas Look[2,3], Tannaz Goodarzi[1], Tim Clarner[4], Miriam Scheld[4], Markus Kipp[5], Eva Verjans[1], Svenja Böll[1], Christopher Neullens[1], Ivan Costa[6], Zhijian Li[6], Lin Gan[7], Bernd Denecke[7#], Angela Schippers[1], Stefan Floess[8], Jochen Huehn[8], Edgar Schmitt[9], Tobias Bopp[9], Hermann Wasmuth[10], Ron Winograd[10], Rudi Beyaert[11,12], Bart Lambrecht[11,13], Martin Zenke[2,3], Norbert Wagner[1], Kim Ohl[1, §], Klaus Tenbrock[1, 14§*]

[1]Dept. of Pediatrics, RWTH Aachen University

[2]Institute for Biomedical Engineering, Department of Cell Biology, RWTH Aachen, University Hospital, Aachen, Germany

[3] Helmholtz Institute for Biomedical Engineering, RWTH Aachen University, Aachen, Germany.

[4]Institute of Neuroanatomy and JARA-BRAIN, Faculty of Medicine, RWTH Aachen University

[5]Institute of Anatomy, Medical University of Rostock, Rostock, Germany

[6]Instutute for Computational Genomics, IZKF, RWTH Aachen University

[7]Genomics Facility, Interdisciplinary Center for Clinical Research Aachen (IZKF Aachen), RWTH Aachen University, Aachen, Germany

[8]Department of Experimental Immunology, Helmholtz Centre for Infection Research, Braunschweig, Germany

[9]Institute for Immunology, University Medical Center, Johannes Gutenberg University Mainz, Mainz, Germany

[10]Luiusenhospital Aachen, Dept. of Medicine, Aachen, Germany

[11]VIB Center for Inflammation Research, Ghent, Belgium

[12]Department of Biomedical Molecular Biology, Ghent University, Ghent, Belgium

[13]Department of Respiratory Medicine, Ghent University Hospital, Ghent, Belgium

[14]Division of Pediatric Rheumatology, Department of Pediatrics, Inselspital, Bern University Hospital, University of Bern, Switzerland

§equal contribution

*Corresponding author: Klaus Tenbrock, Dept. of Pediatrics, RWTH Aachen University, Pauwelsstraße 30, 52074 Aachen, ktenbrock@ukaachen.de, 0049-2418089140

#Bernd Denecke unfortunately passed away during the project

The authors have declared that no conflict of interest exists.

ABSTRACT

Regulatory T cells (T_{regs}) are gatekeepers of immune homeostasis and characterized by expression of Foxp3, which maintains T_{reg} identity. Here we demonstrate that in mice with a Foxp3-specific knockout of CREB, enhanced numbers of T_{regs} are found *in vivo* in spleen, lung and colon. These T_{regs} display a reduced Foxp3 expression, but enhanced expression of the IL-33 receptor (ST-2), IL-10, IL-13, and CREM. CREB deficient T_{regs} were highly suppressive *in vitro* and prevented disease activity in CD4 T cell mediated transfer colitis in an IL-10 dependent way. Mechanistically CREB fulfils dual roles in T_{regs}. First it downregulates Foxp3 expression, however in cooperation with CREM, CREB expression in T_{regs} alters chromatin accessibility to the ST-2 region and thereby influences T cell specific immune responses mediated by IL-10.

Brief summary: Mice with a Foxp3-specific knockout of CREB display enhanced expression of IL-13, IL-10, ST-2 and CREM, which prevents gut inflammation

61 GRAPHICAL ABSTRACT

62

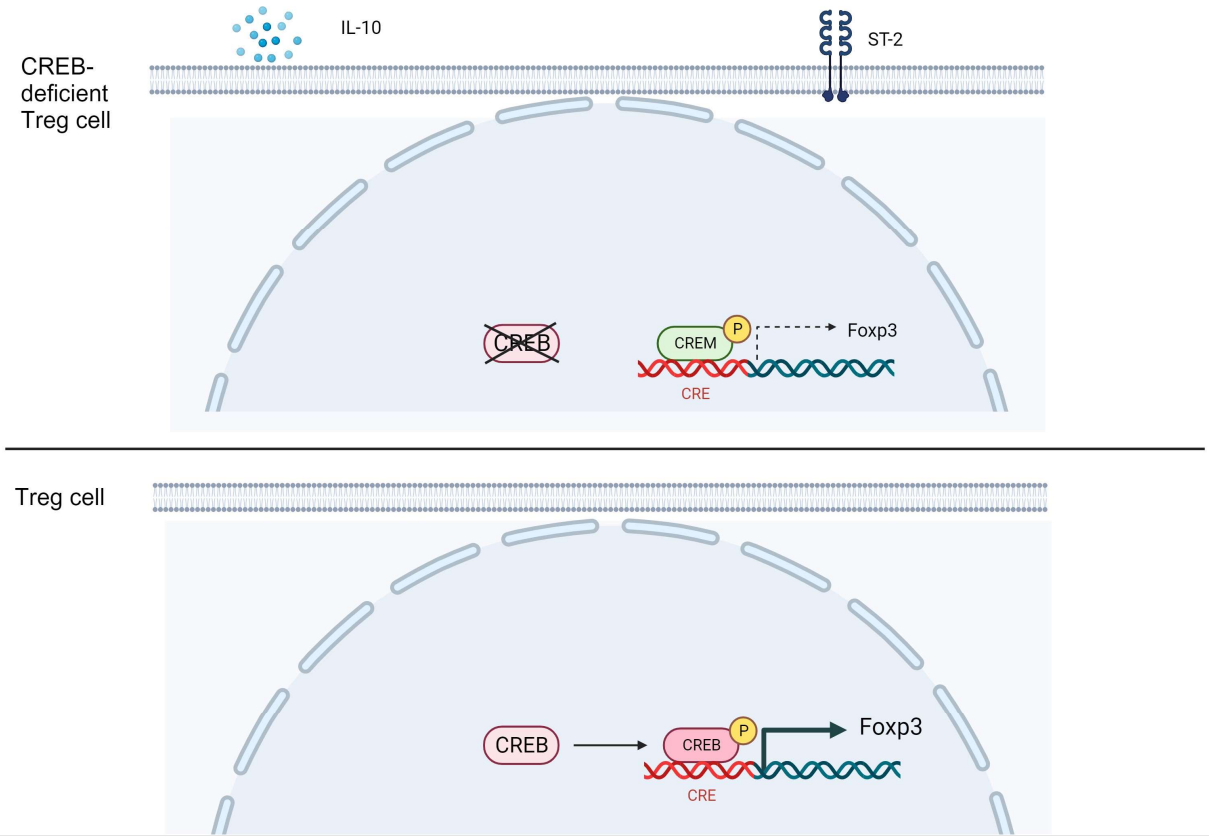

63

64 **Created by Biorender**

65

66

67

68

69

70

71

72

73

74

1 INTRODUCTION

Regulatory T cells (T_{regs}) are important for the maintenance of immune homeostasis and characterized by expression of Foxp3. Loss of Foxp3 results in a devastating autoimmune syndrome in mice (scurfy disease)(Wildin, Ramsdell et al. 2001) and humans (IPEX, polyglandular autoimmunopathy) (Bennett, Christie et al. 2001). Two sources of Foxp3$^+$ cells have been described, one of which is located to the thymus, "thymus-derived T_{regs}" (tT_{regs}), and the second to the periphery, where conventional CD4$^+$ T cells can convert into Foxp3$^+$ "inducible T_{regs}" (iT_{regs}) after T cell stimulation in the presence of TGF-β (Zhou, Bailey-Bucktrout et al. 2009). tT_{reg}-cell as well as iT_{reg} cell generation largely depend on the presence of IL-2 which is not only required for homeostatic maintenance but also for the thymic development of T_{regs} (Setoguchi, Hori et al. 2005, Zorn, Nelson et al. 2006, Liao, Lin et al. 2011, Ohl and Tenbrock 2015).

ST-2 also known as IL1RL1 belongs to Toll-like receptor/IL-1 receptor superfamily. ST-2 through its ligand IL-33 plays a pivotal role in MyD88/ NFκB signaling. The interaction of ST-2 with its ligand IL-33 induces Foxp3 and GATA3 expression in T_{regs} in particular at mucosal sites (Schiering, Krausgruber et al. 2014). ST-2 mainly exists in two isoforms; soluble ST-2 (sST-2) and membrane bound ST-2. sST-2 functions as a decoy receptor of IL-33 and inhibits NFκB signaling, while membrane bound ST-2 promotes NFκB signaling (Kakkar and Lee 2008). It has been shown that increased ST-2 levels were observed in diseases like inflammatory bowel disease (IBD), Asthma, colon cancers, and Graft versus Host disease (Griesenauer and Paczesny 2017). In many non-lymphoid tissues, T_{regs} show enriched expression of the ST-2 and most of these are iT_{regs}. The regulation of the ST-2$^+T_{regs}$ is dependent on the transcription factor Basic leucine zipper transcription factor ATF-like (BATF) (Delacher, Imbusch et al. 2017, Delacher, Imbusch et al. 2020), while other factors which have not been defined yet. BATF belongs to the cAMP responsive element binding protein/activating transcription factor (CREB/ATF) family of transcription factors, is able to dimerize with Jun

101 and has been shown to compete with CREB for binding to CRE/AP1 sites (Dorsey, Tae et al.
102 1995, Manna and Stocco 2007).

103 The accessibility of the *Foxp3* gene promoter, as well as other cis-regulatory elements in the
104 *Foxp3* locus are under tight epigenetic control, especially by histone acetylation, methylation
105 and cytosine-phospho-guanosine (CpG-)DNA methylation (Lal and Bromberg 2009). The
106 *Foxp3* gene contains a highly conserved CpG-rich region in the first intron (+4201 to +4500)
107 which appears to be critical in *Foxp3* gene regulation. CpG residues in this region are
108 completely methylated (thus resulting in a "silenced" gene locus) in non-T_{regs} ($CD4^+CD25^-$) and
109 fully de-methylated ("open, accessible" gene locus) in tT_{regs} ($CD4^+CD25^+$) in mice and humans,
110 for which this region was termed T_{reg}-specific de-methylated region (TSDR) (Baron, Floess et
111 al. 2007, Floess, Freyer et al. 2007, Kim and Leonard 2007). The TSDR possesses
112 transcriptional enhancer activities and transcription factors c-Rel, Ets-1 and those of the
113 CREB/ATF family have been identified to bind and trans-activate the de-methylated TSDR
114 (Floess, Freyer et al. 2007, Kim and Leonard 2007, Polansky, Schreiber et al. 2010). Thus,
115 CREB was identified previously as a positive regulator of Foxp3 expression *in vitro*.
116 Through yet-to-be-defined mechanisms, T_{regs} loose Foxp3 expression and become pro-
117 inflammatory effector cells under certain conditions (Tsuji, Komatsu et al. 2009, Zhou, Bailey-
118 Bucktrout et al. 2009). In detail the loss of Foxp3 expression results in T_{h1}, T_{h17} and T follicular
119 helper (T_{fh}) conversion of T_{regs}, while a reduction of Foxp3 expression leads to a T_{h2} conversion
120 of tT_{regs} (Wang, Souabni et al. 2010). Therefore, additional molecular events might complement
121 Foxp3 function in the generation of T_{regs} and the maintenance of their function and phenotype.
122 DNA methylation is one of the important epigenetic regulations to control transcription. As
123 mentioned above, methylation patterns of Foxp3 promoter and enhancer regions have been
124 intensively investigated in the past years. In addition, a paper by the group of Feuerer showed

125 tissue specific regulation of DNA methylation in T_{regs} also regarding other loci including gene
126 sites that are associated with the T_{h2} subset (Delacher, Imbusch et al. 2017).
127 Our understanding of molecular mechanism of suppression is still limited. T_{regs} control immune
128 activation by acting directly or indirectly on effector CD4 and CD8 T cells and antigen-
129 presenting cells. Cyclic AMP (cAMP) is long known as a potent suppressor of T cell activation
130 and function. T_{regs} generate and accumulate high levels of cAMP, which can be transferred into
131 target cells as one mechanism of suppression (Bopp, Becker et al. 2007, Bodor, Bopp et al.
132 2012). Indirect mechanisms include the secretion of cytokines, such as IL-10, IL-35 and TGF-
133 ß. IL-10 plays an important role in suppressing $CD4^+$ effector T-cell function. Additionally,
134 IL-10 prevents activation of antigen-presenting cells (APCs), such as dendritic cells and
135 macrophages, by downregulation of costimulatory molecules and production of inflammatory
136 cytokines within these cells (Okamoto, Fujio et al. 2011). Selective ablation of IL-10 in $Foxp3^+$
137 T_{regs} revealed that IL-10 production by T_{regs} is essential for keeping the immune response in
138 check at environmental interfaces such as colon and lungs (Rubtsov, Rasmussen et al. 2008).
139 IL-10 also acts in an autocrine manner by maintaining FoxP3 expression and the suppressive
140 capacity of T_{regs} (Murai, Turovskaya et al. 2009, Unutmaz and Pulendran 2009). Interestingly,
141 IL-10 is responsive to cAMP stimulation at least in THP1 cells and macrophages and the IL-10
142 promoter contains four putative cAMP response element sites (CRE, TGACGTCA) sites, which
143 are conserved between men and mice (Brenner, Prosch et al. 2003). Following TLR activation,
144 pCREB (phosphorylated CREB) is recruited to the IL-10 promoter and enhances IL-10
145 transcription in macrophages (Sanin, Prendergast et al. 2015).
146 CREB is a phosphorylation-dependent transcription factor that is involved in several cellular
147 processes, amongst others proliferation and cell survival. CREB and CREM belong to the
148 CREB/activating transcription factor (ATF) family. Hallmark of which is a conserved basic
149 region/leucine zipper (bZIP) domain, which binds to an 8-base pair palindromic DNA sequence,
150 called CRE site (Foulkes, Borrelli et al. 1991, Sassone-Corsi 1995, De Cesare and Sassone-

151 Corsi 2000). The transactivation domain is required for the recruitment of CREB binding
152 protein (CBP/p300), which has histone-acetylating (HAT) activities. CREM has many
153 alternative splice variants. ICER is a splice variant of CREM that lacks transcriptional
154 activation domains and thereby functions as a repressor of cAMP-induced CRE-mediated
155 transcription. CREMα also lacks both Q-domains. The Q2 domain is needed to activate HAT
156 activities of p300 and CBP and CREMα is therefore unable to promote HAT activities of p300
157 and CBP (Asahara, Santoso et al. 2001). ICER also has an alternative transcription initiation
158 site and is induced by a unique alternative promoter (Foulkes, Borrelli et al. 1991). ICER has
159 been described as central to Th17 cell differentiation in autoimmunity (Yoshida, Comte et al.
160 2016). On the other hand, Bodor et al. showed that ICER is important for cAMP-driven Treg-
161 cell suppression mechanism in activated T cells (Bodor, Bopp et al. 2012). Expression of
162 CREMα, a repressor isoform of CREM, is increased in $CD4^+$ T cells from SLE patients, and
163 forced expression of CREMα in human T cells enhances IL-17A expression (Rauen, Hedrich
164 et al. 2011). Moreover, mice overexpressing CREMα in T cells display increased IL-17
165 production and severe skin inflammation, as well as mild lupus-like disease (Lippe, Ohl et al.
166 2012). In addition, we have shown that CREMα actively recruits a histone deacetylase
167 (HDAC1) to promote chromatin condensation (Tenbrock, Juang et al. 2006). As a third
168 mechanism CREMα recruits the DNA methyltransferase DNMT3a, which promotes
169 methylation of DNA and thereby represses the binding of transcription factors resulting in
170 closure of chromatin (Hedrich, Rauen et al. 2011). CREMα itself can furthermore bind to the
171 aforementioned CRE within the *Il2* promoter (Powell, Lerner et al. 1999), (Lippe, Ohl et al.
172 2012, Ohl, Wiener et al. 2015). The group of George Tsokos demonstrated that SLE T cells
173 have a decreased ability to produce IL-2 in response to stimulation with antigens (Via, Tsokos
174 et al. 1993), which is related to enhanced T cellular expression of CREMα in these patients and
175 an aberrant CREM/CREB ratio (Solomou, Juang et al. 2001). CREB binds to a CRE site within

176 the proximal *IL2* promoter resulting in enforced *IL2* transcription. Mice expressing a dominant
177 negative (inactive) CREB isoform show a markedly decreased production of IL-2. Additionally,
178 $CREB^{-/-}$ mice die prenatally while they display a severely impaired T cell development (Barton,
179 Muthusamy et al. 1996).
180 Previous data from Wang et al., group suggested that CREB negatively regulated the survival
181 of iT_{regs} and is particularly important in the generation of CD4+Th17 cells. Using $CD4^{CRE}$
182 $CREB^{fl/fl}$ mice they showed that these cells prevented colitis in a $Rag2^{-/-}$ model, however their
183 model has the disadvantage that CD4 cells of these mice are expressing lower amounts of IL-2
184 that could hamper iT_{reg} induction. Our analysis now expands their findings and determines an
185 important tole for CREB in the generation of ST2+T_{regs}. Using $Foxp3^{CRE}CREB^{fl/fl}$ mice we
186 herein confirm the colitis phenotype but can show that i) CREB deficiency in T_{regs} induces
187 expression of ST2+T_{regs}, ii) the phenotype that prevents colitis in $Rag2^{-/-}$ mice is primarily
188 dependent on abundance of IL-10, iii) and that this phenotype can be reversed by knockout of
189 CREM that lowers the expression of ST2.
190
191
192
193
194
195
196
197
198

199 # 2 MATERIAL AND METHODS

200 ## 2.1 Mice strains

201 Experiments were performed with age matched *CREB*$^{fl/fl}$ and *Foxp3*^{cre}*CREB*$^{fl/fl}$ mice (all
202 C57BL/6). *Foxp3*^{cre}*CREB*$^{fl/fl}$ mice were generated by crossing CREB-flox mice (Okawa,
203 Motohashi et al. 2006) with C57BL/6 Foxp3-IRES Cre mice (provided by T. Bopp, University
204 of Mainz). *Foxp3*$^{cre-}$*CREB*$^{fl/fl}$ mice were used as controls (denoted as *CREB*$^{fl/fl}$).
205 Foxp3^{Cre}ROSA^{RFP} were provided by T. Bopp University of Mainz and crossed with our
206 *CREB*$^{fl/fl}$ mice. Rag2$^{-/-}$ (C57BL/6) mice were provided by A. Schippers (Uniklinik RWTH
207 Aachen). All mice were bred in our animal facility and kept under standardized conditions.

208 ## 2.2 Transfer colitis

209 To induce transfer colitis, Rag2$^{-/-}$ mice were adoptively transferred with 2 x 10^6 CD4$^+$ CD25$^-$ T
210 cells. Animals were sacrificed as soon as a significant loss of weight was measurable. Spleen
211 and mLNs were harvested for further analysis. One part of the colon was fixed in formalin for
212 histological scoring and the other part was fixed in RNAlater (Qiagen, Germany) for subsequent
213 mRNA analysis. For soluble ST2 (sST2) treatment, mice received 100 µg mouse sST2
214 (produced by the VIB Protein Core facility and provided by R. Beyaert, VIB-UGent Center for
215 Inflammation Research), three times/week by intraperitoneal means (i.p). Control group
216 received PBS i.p. For IL-10R treatment, mice received 500 µg anti IL-10R antibody (1B1mAB)
217 (kindly provided by Prof. Edgar Schmitt, University of Mainz) or IgG control AK (Rat IgG
218 kappa) i.p. once a week during the first three weeks.

219 ## 2.3 Histological scoring

220 4 µm paraffin sections from the fixed colon were cut serially, mounted onto glass slides, and
221 deparaffinized. The colon sections were stained with hematoxylin and eosin by the Core Facility
222 (IZKF) of the RWTH Aachen University. Blinded histological scoring was performed using a
223 standard microscope, based on JLS method as described previously (Bleich, Mahler et al. 2004,
224 Pils, Bleich et al. 2011). Each colon section was scored for the four general criteria: severity,
225 degree of hyperplasia, degree of ulceration, if present, and percentage of area involved. A

226 subjective range of 1-3 (1 = mild, 2 = moderate, 3 = severe) was used for the first three
227 categories. Severity: Focally small or widely separated multifocal areas of inflammation limited
228 to the lamina propria were graded as mild lesions (1). Multifocal or locally extensive areas of
229 inflammation extending to the submucosa were graded as moderate lesions (2). If the
230 inflammation extended to all layers of the intestinal wall or the entire intestinal epithelium was
231 destroyed, lesions were graded as severe (3). Hyperplasia: Mild hyperplasia consisted of
232 morphologically normal lining epithelium that was at least twice as thick (length of crypts) as
233 adjacent or control mucosa. Moderate hyperplasia was characterized by the lining epithelium
234 being two- or three-times normal thickness, cells were hyperchromatic, numbers of goblet cells
235 were decreased, and scattered individual crypts developed an arborizing pattern. Severe
236 hyperplastic regions exhibited markedly thickened epithelium (four or more times normal
237 thickness), marked hyperchromasia of cells, few to no goblet cells, a high mitotic index of cells
238 within the crypts, and numerous crypts with arborizing pattern. Ulceration was graded as: 0 =
239 no ulcer, 1 = 1-2 ulcers (involving up to a total of 20 crypts), 2 = 1-4 ulcers (involving a total
240 of 20-40 crypts), and 3 = any ulcers exceeding the former in size. A 10% scale was used to
241 estimate the area involved in the inflammatory process. 0 = 0%, 1 = 10%-30%, 2 = 40%-70%,
242 3 = >70%.

243 ## 2.4 Cell isolation

244 Single cell suspensions were isolated from spleens and LNs (pLN and mLNs) using cell
245 strainers and erythrocytes were lysed with lysis buffer. To obtain immune cells from lung, tissue
246 was excised into small pieces and was digested with 0.1% collagenase in DPBS for 1hr. The
247 digested fraction was passed through a 40µm nylon strainer and rinsed with DPBS. The flow
248 through was centrifuged and the cell pellet was lysed using RBC lysis buffer. The cell pellet
249 was used for the Flow cytometric analysis. Colon was retrieved from the mice and rinsed with
250 a cannula with PBS+0.5%BSA. Afterwards colon was excised into small pieces and placed in
251 a digestive medium containing RPMI (10ml), Collagenase V (0.85mg/ml), Collagenase D

252 (1.25mg/ml), Dispase (1mg/ml) and DNase (30µg/ml) and incubated for 45 minutes at 37°C
253 with gentle shaking. The digested fraction was passed through a 40um nylon strainer and the
254 flow through was collected and centrifuged to obtain a pellet. Percoll gradient centrifugation
255 was performed by using 35% percoll and centrifugation was performed. The cell pellet obtained
256 was lysed using RBC lysis buffer and is used for further analysis. Liver was retrieved from the
257 mice. Gall bladder was removed and liver was excised into small pieces and was placed in a
258 digestive medium containing RPMI without FCS (3ml), 1.25mg/ml Collagenase D and 30µg/ml
259 DNase. The fraction was incubated for 45 minutes and digestion was stopped by adding
260 PBS+0.5% BSA+2mM EDTA and homogenized using a syringe. The digested fraction was
261 passed through a 100µm nylon strainer and the flow through was centrifuged. The pellet
262 obtained was used for the percoll gradient centrifugation by using 35% percoll. The cell pellet
263 obtained after the percoll gradient centrifugation was lysed using RBC lysis buffer and is used
264 for flow cytometric analysis.

265 2.5 T cell differentiation assays

266 MACS isolated $CD4^{+}CD25^{-}$ T cells ($2x10^{6}$ per ml) were incubated with plate-coated anti-CD3
267 (10µg/ml, eBioscience) and soluble anti-CD28 (1µg/ml) (eBioscience). T_H0 cells were left
268 without exogenous cytokines, 5 ng/ml TGF-β was added to induce T_{reg} differentiation.

269 2.6 Flow cytometry

270 For surface staining, single cell suspensions were stained with anti-CD4, anti-CD3, anti-CD8,
271 anti-B220, anti-CD25, CD45, anti-GL-7, anti-ICOS, anti-ST2, anti-Nrp1, anti-PD-1 (all from
272 eBioscience, Germany). For intracellular staining of CREB, Foxp3, CTLA-4, Helios, GATA3,
273 T-bet and RORγt, cells were fixed and permeabilized with a FOXP3 staining buffer set
274 (Thermofischer, eBioscience, Germany) following the manufacturer's instructions and stained
275 with respective antibodies (eBioscience, Germany) for 30 min. Intracellular cytokines were
276 stained with anti-IFN-γ-Alexa 647 (eBioscience) and anti-IL-17-Alexa 488 (BD), and IL-10-
277 APC (ebiosciences) after PMA (30nM) and Ionomycin (1.5µM) (both Sigma-Aldrich, USA)

278 re-stimulation in the presence of GolgiPlug/GolgiStop (BD Biosciences). A daily calibrated
279 FACS-Canto II flow cytometer (Becton Dickinson, MountainView, CA) was used to perform
280 phenotypic analysis. Lymphocytes were gated by forward (FSC), side scatter (SSC), and CD3,
281 CD4, B220 expression. A figure exemplifying the gating strategies is provided in the
282 Supplementary Information (**Supp. Fig. 5**). For data analysis FCS-Express 4.0 Research
283 Edition (DeNovo software Glendale, CA, USA) and FlowJo version 10 were used.

284 2.7 Luciferase Assay

285 RLM cells carrying a stable pGL3-TSDR-FoxPro luciferase plasmid were kindly provided by
286 Jochen Huehn (HZI Braunschweig). Cells were transfected with pcDNA-CREB plasmid or
287 pcDNA. Cells were left to rest over night before luciferase activity was measured by using the
288 Dual-Glo Luciferase Assay System (Promega, USA).

289 2.8 RNA isolation and real-time PCR

290 Total RNA from isolated T cells and colon tissue was isolated using the RNeasy Mini Kit
291 (Qiagen, Germany). cDNA was then generated from 200 ng total RNA using the RevertAid H
292 Minus First Strand cDNA Synthesis Kit (Thermo Fisher Scientific, USA) according to the
293 manufacturer´s instructions. RT-PCR was performed using the SYBR Green PCR kit
294 (Eurogentec, Germany) and data were acquired with the ABI prism 7300 RT-PCR system
295 (Applied Biosystems / Life Technologies, Germany). Each measurement was set up in
296 duplicate. After normalization to the endogenous reference control gene ß-actin for mice, the
297 relative expression was calculated.

298 2.9 RNA extraction and microarray for gene expression analysis

299 $CD4^{+}CD25^{+}Nrp1^{+}$ T_{regs} were sorted by FACS. Genome wide transcriptome analyses of
300 $Foxp^{cre}CREB^{fl/fl}$ and $CREB^{fl/fl}$ T_{regs} were performed in independent triplicates using Gene Chip®
301 Mouse Gene 2.0 arrays (Affymetrix, Santa Clara, CA, USA). Total RNA extraction was carried
302 out using the RNeasy Micro Kit (Qiagen, Germany) according to manufacturer's protocol and
303 then quantified (Nanodrop). RNA quality was assessed using the RNA 6000 Nano Assay with

304 the 2100 Bioanalyzer (Agilent, Santa Clara, CA, USA). Samples for the Gene 2.0 arrays were
305 prepared and hybridized to the arrays according to the Affymetrix WT Plus Kit manual. Briefly,
306 for each sample, 100 ng of total RNA was reversed transcribed into cDNA using a random
307 hexamer oligonucleotide tagged with a T7 promoter sequence. After second strand synthesis,
308 double strand cDNA was used as a template for amplification with T7 RNA polymerase to
309 obtain antisense cRNA. Random hexamers and dNTPs spiked out with dUTP were then used
310 to reverse transcribe the cRNA into single stranded sense strand cDNA. The cDNA was then
311 fragmented with uracil DNA glycosylase and apurinic/apyrimidic endonuclease 1. Fragment
312 size was checked using the 2100 Bioanalyzer and ranged from 50 to 200 bp. Fragmented sense
313 cDNA was biotin-endlabeled with TdT and probes were hybridized to the Gene 2.0 arrays at
314 45 °C for 16h with 60 rpms. Hybridised arrays were washed and stained on a Fluidics Station
315 450 (program: FS450 0002) and scanned on a GeneChip® Scanner 3000 7G (both Affymetrix).
316 Raw image data were analyzed with Affymetrix® Expression Console™ Software (Affymetrix,
317 USA), and gene expression intensities were normalized and summarized with a robust
318 multiarray average algorithm(Irizarry, Hobbs et al. 2003). Transcripts that were expressed
319 differently more than 1.5-fold with a raw p-value lower than 0.05 between the sample groups
320 were categorized as regulated. Enrichment analysis for Wiki pathways was performed using
321 WebGestalt (Wang, Duncan et al. 2013). For the enrichment analysis only, genes changed at
322 least 1.5-fold with a p-value lower than 0.05 between *Foxp3*^{cre}*CREB*$^{fl/fl}$ and *CREB*$^{fl/fl}$ samples
323 were taken into consideration.

324 ## 2.10 TSDR Methylation analysis

325 For all methylation analyses, cells from male mice were used. Genomic DNA was prepared
326 from FACS-sorted T_{conv} cells ($CD4^+CD25^-$) as well as T_{reg} cells ($CD4^+CD25^+Nrp1^+$) from
327 *CREB*$^{fl/fl}$ and *Foxp3*^{cre}*CREB*$^{fl/fl}$ mice and subsequently converted by bisulfite according to the
328 manufacturer's instructions (DNeasy Blood & Tissue Kit, Qiagen; EZ DNA Methylation-
329 Lightning Kit, Zymo Research). Pyrosequencing of the Treg cell-specific demethylated region

330 (TSDR) (chromosome position X:7583950-7584149, genome assembly GRCm38.p6) was
331 performed as described previously (Garg, Muschaweckh et al. 2019).

332 ## 2.11 ATAC Seq

333 Omni-ATAC-seq was performed according to (Corces, Trevino et al. 2017, Li, Schulz et al.
334 2019) with minor modifications. Prior to transposition, dead cells were removed by
335 centrifugation (800 rpm, 4 min, 4°C). The transposition reaction was with 7.5 µL Tagment
336 DNA Enzyme 1 (TDE1) for 60 'min at 37°C. Pre-amplification was with NEBNext Ultra II Q5
337 Master Mix and Nextera PCR Primers (5 cycles). Quantitative PCR amplification was with
338 NEBNext Ultra II Q5 Master Mix, Nextera PCR Primer and SYBR Gold to determine the
339 number of additional cycles. PCR amplification of additional cycles was as for pre-
340 amplification. PCR fragments were purified with Qiagen MinElute PCR Purification Kit and
341 library concentration and quality were determined by Agilent High Sensitive DNA Kit and
342 TapeStation, respectively. ATACseq libraries were sequenced on the Illumina NextSeq 500
343 Platform with 75 bps paired end reads in duplicates. ATAC-seq libraries were trimmed with
344 Trim Galore (parameters -q 30 –paired –trim1) and aligned to mouse genome (mm9) using
345 Bowtie2 (Langmead and Salzberg 2012) (parameters -X2000 –no-mixed –no-discordant).
346 Duplicates fragments were removed, and reads were filtered for alignment quality of >Q30
347 using samtools (Li, Handsaker et al. 2009). Next, we use MAC2 (Zhang, Liu et al. 2008) to
348 perform peak calling (parameters –nomodel –nolambda –keep-dup auto –call-summits).
349 Transcription factor footprinting and differential activity was performed using HINT-ATAC as
350 described in (Li, Schulz et al. 2019).

351 ## 2.12 ELISA

352 Total IgG and IgE was measured from sera using the the Ready-set-go ELISA system
353 (affymetrix: eBioscience, USA). IL-10 was determined in cell supernatants using Mouse IL-10
354 ELISA Ready-SET-GO! (2nd Generation), Thermo Fisher Scientific according to
355 manufacturer's instructions.

2.13 Statistical analysis

All data are presented as mean ± standard error (SEM). Data were tested for normality using Shapiro-Wilk Normality test. Differences between two groups were evaluated using two-tailed unpaired or paired (if indicated), Student's t-test. A two-tailed Mann Whitney test was used, if data were not normally distributed. ONE-way ANOVA was performed if there are more than two groups. Measurements were taken from distinct samples. All statistical analysis and subsequent graphics generation were performed using GraphPad Prism version 7.0 and 8.0 (GraphPad Software, USA). A p-value <0.05 was statistically significant.

2.14 Study approval

The animal study was approved by the regional government authorities and animal procedures were performed according to German legislation for animal protection. Permission for the projects was granted by the Regierungspräsident/LANUV Nordrhein-Westfalen (81-02.04. 2017.A393).

2.15 Data availability

The ATAC-Seq and microarray raw datasets have been deposited in GEO under the accession codes GSE157693 and GSE157933. All data that support the findings of this study are available within the article and Supplementary Files. All other data, including raw data used in each figure will be provided upon reasonable request to the corresponding author.

375 # 3 RESULTS

376 ## 3.1 CREB enhances T_{reg} numbers but downregulates Foxp3 expression in T_{regs}

377 CREB is a transcriptional activator and has been described to critically stabilize Foxp3
378 expression (Kim and Leonard 2007). It is therefore widely accepted that CREB promotes FoxP3
379 expression in T_{regs} (Ruan, Kameswaran et al. 2009, Polansky, Schreiber et al. 2010, Zheng,
380 Josefowicz et al. 2010). To verify this hypothesis in vivo, we generated mice with a Foxp3-
381 specific knockout of CREB (*Foxp3^{cre}CREB$^{fl/fl}$*). To our surprise, these mice showed enhanced
382 numbers of CD25^{+}/Foxp3^{+} positive T_{regs} in thymus (**Fig. 1A and D**), spleen (**1B and D**) and
383 peripheral lymph node (pLN) **(Fig. 1C and D**). Splenic T_{regs} showed no altered expression of
384 Nrp1, PD-1, CTLA4, and ICOS (**Supp Fig. 1A-B**). There was also no convincing different
385 expression of T_h lineage transcription factors GATA3 and RORyT and T-bet in CD4^{+}Foxp3^{+}
386 cells within different organs (**Supp. Fig. 2A-E)**. However, *Foxp3^{cre}CREB$^{fl/fl}$* mice displayed
387 lower Foxp3 expression in T_{regs} on the single cell level (**Fig. 1E and F**) which can be explained
388 by the fact that CREB directly activates the TSDR (Kim and Leonard 2007) (**Fig. 1G**). To
389 verify Cre expression in the Foxp3-Cre mice, we crossed *Foxp3^{cre}CREB$^{fl/fl}$* mice with a Cre-
390 inducible reporter mice (*ROSA^{RFP}*) and examined reporter gene expression in lymphocytes. RFP
391 expression was confined to CD4^{+}CD25^{+} cells, which is of importance to exclude cell extrinsic
392 side-effects (**Fig. 1H and I**).

393 We further used *Foxp3^{cre}CREB$^{fl/fl}$ ROSA^{RFP}* mice to assess percentages of T_{regs} in non-lymphoid
394 organs. While we did not observe differences in liver tissue, we found a particularly marked
395 upregulation of T_{reg} percentages within lungs and colon of *Foxp3^{cre}CREB$^{fl/fl}$ ROSA^{RFP}* mice
396 compared to *Foxp3^{cre}ROSA^{RFP}* mice (**Fig. 1J -L**) and enhanced absolute numbers of T_{regs} in
397 colon of Foxp*3^{cre}CREB$^{fl/fl}$ ROSA^{RFP}* (**Supp. Fig. 7B**). This prompted us to analyse if CREB
398 expression in T_{regs} differs in different tissues. We could not find an association of high tissue
399 dependent CREB expression and effects of CREB deficiency on T_{reg} percentages, however
400 found a quite high expression of CREB in murine colon T_{regs} (**Supp. Fig. 8**).

401 ### 3.2 CREB-deficient T_{regs} are suppressive *in vitro*

402 To test if lower Foxp3 expression affects suppressive capacity of CREB deficient T_{regs}, we co-
403 cultured *CREB*$^{fl/fl}$ T_{regs} and *Foxp3*^{cre}*CREB*$^{fl/fl}$ T_{regs} with anti-CD3 and anti-CD28 stimulated WT
404 CD4^{+} cells. Surprisingly, *Foxp3*^{cre}*CREB*$^{fl/fl}$ T_{regs} revealed an even enhanced capacity to reduce
405 CD4^{+} T cell proliferation (**Fig. 2A and B**). These data suggest that deletion of CREB, despite
406 reducing Foxp3 expression per cell, enhances function of T_{regs}. In addition, expression of Helios
407 was enhanced (**Fig. 2C**) and bisulfite sequencing revealed a demethylated TSDR (**Fig. 2D**),
408 which suggests a stable and suppressive phenotype (Thornton, Lu et al. 2019). In conclusion,
409 despite reduction of Foxp3 levels per cell, CREB deficiency leads to stable and functional T_{regs}
410 *in vitro*.

411 ### 3.3 CREB deficient T_{regs} reveal gene expression signature with enhanced expression of
412 IL-10, IL-4, IL-13 and ST2

413 To understand why CREB deficient T_{regs} are suppressive despite reduced Foxp3 expression, we
414 performed a whole transcriptome analysis (Affymetrix HTA2 arrays) of flow sorted
415 (CD4^{+}CD25^{+}Nrp-1^{+}) *Foxp3*^{cre}*CREB*$^{fl/fl}$ and *CREB*$^{fl/fl}$ T_{regs} (**Supp. Fig. 3A**) and appropriate
416 wild-type mice because at the time of this analysis the *Foxp3*^{CRE}*CREB*$^{fl/fl}$ *ROSA*^{RFP} mice were
417 not yet available. Using a fold–change of 1.5 and a p-value of less than 0.05 we found 111
418 downregulated and 122 upregulated genes in the *Foxp3*^{cre}*CREB*$^{fl/fl}$ compared to *CREB*$^{fl/fl}$ T_{regs},
419 among those were IL-10 and IL-13 the 2 most strongly upregulated in the *Foxp3*^{cre}*CREB*$^{fl/fl}$ T_{regs}
420 (**Fig. 3A**). KEGG pathway analysis revealed an enrichment of differentially regulated genes in
421 pathways that are associated with Th2 cytokines, such as asthma, Th2 and Th2 cell
422 differentiation and cytokine-cytokine receptor interaction pathways (**Fig. 3B**). Higher *Il13 and*
423 *Il10* mRNA expression in *Foxp3*^{cre}*CREB*$^{fl/fl}$ T_{regs} could be further confirmed by RT-qPCR (**Fig.**
424 **3C** and **D**). CD4^{+}CD25^{+}Foxp3^{+} cells also showed enhanced IL-10 protein levels after 3 days of
425 CD3/CD28 stimulation as assessed by flow cytometry (**Fig. 3E and F**). *In vitro* T_{reg}
426 differentiation with TGF-β revealed a reduced capacity of *Foxp3*^{cre}*CREB*$^{fl/fl}$ T cells to
427 differentiate towards Foxp3^{+} cells, while IL-10 expressing cells within Foxp3^{+} cells were

428 enhanced. Furthermore IL-10 cytokine expression of TGF-β stimulated *Foxp3^{cre}CREB$^{fl/fl}$* T
429 cells measured by ELISA was enhanced as well as *Il13, Il5 and Il10* mRNA expression, which
430 suggests that CREB deficiency in T_{regs} induces a Th2 biased phenotype (**Fig. 3H-L**). Beyond
431 cytokines, expression of Il1r1 (ST2) showed enhanced expression on the microarray. ST2, the
432 receptor of IL-33 is preferentially expressed on colonic T_{regs}, where it promotes T_{reg} function
433 and adaption to the inflammatory environment. It provides a necessary signal for T_{reg}-cell
434 accumulation and maintenance in inflamed tissues, and it was shown to regulate IL-10
435 expressing T_{regs} in the gut (Schiering, Krausgruber et al. 2014). In addition, IL-33 has been
436 identified as a major interleukin in asthma pathology (Drake and Kita 2017). ST2 was highly
437 expressed in the *Foxp3^{cre}CREB$^{fl/fl}$* T_{regs}, which was confirmed by flow cytometry (**Fig. 3M and**
438 **N**). Moreover, the whole transcriptome analysis also revealed an upregulated expression of
439 CREM in *Foxp3^{cre}CREB$^{fl/fl}$* T_{regs} and qRT-PCR also showed tendentially enhanced CREM
440 expression in *Foxp3^{cre}CREB$^{fl/fl}$* T_{regs} **(Fig. 3O)**. In conclusion, these data suggest that CREB
441 deletion induces ST2^{+} T_{regs}. This finding led us to investigate the protein expression of ST2
442 within different organs in *Foxp3^{cre}ROSA^{RFP}* and *Foxp3^{cre}CREB$^{fl/fl}$ROSA^{RFP}* mice. ST2
443 expression was clearly enhanced in T_{regs} in the thymus, spleen, mesenteric lymph node, lung
444 and colon of these mice **(Fig. 3P-T)**.

445 ### 3.4 *Foxp3^{cre}CREB$^{fl/fl}$* T cells dampen inflammation in experimental colitis

446 Since ST2^{+}T_{regs} also play a protective role in intestinal mucosal inflammation (Schiering,
447 Krausgruber et al. 2014), we performed a transfer of *Foxp3^{cre}CREB$^{fl/fl}$* T cells (CD4+CD25-) or
448 appropriate *CREB$^{fl/fl}$* T cells (CD4+CD25-) into lymphopenic Rag2$^{-/-}$ mice. This usually results
449 into development of colitis within 5 weeks. Strikingly, transfer of *Foxp3^{cre}CREB$^{fl/fl}$* T cells did
450 not result in the expected weight loss (**Fig. 4A**) and recipient mice displayed decreased
451 intestinal inflammation (**Fig. 4B-C**). Furthermore, inflammatory cytokines in the gut were
452 markedly reduced (**Fig. 4D**) as well as IL-17 and IFN-γ production in CD4^{+} T cells in the
453 mesenteric lymph nodes (mLNs) (**Fig. 4E-G**). The experiment was repeated with CD4+CD25-

454 T cells of *Foxp3*^{cre}*ROSA*^{RFP} and *Foxp3*^{cre}*CREB*$^{fl/fl}$ *ROSA*^{RFP} mice into Rag2-/- mice and ending
455 with the same results. The transfer of CD4+CD25- T cells of *Foxp3*^{cre}*CREB*$^{fl/fl}$ *ROSA*^{RFP} mice
456 prevented development of colitis and resulted in enhanced accumulation of RFP+ T_{regs} in
457 different organs (**Fig. 5A-G**). Interestingly, RFP+ T_{regs} also accumulated in the liver, while we
458 did not find a difference in the RFP expression in the *Foxp3*^{cre}*CREB*$^{fl/fl}$ *ROSA*^{RFP} mice under
459 steady state conditions.

460 ## 3.5 Blockade of IL-10 but not of ST2 signalling reverses protective effects of
461 *Foxp3*^{cre}*CREB*$^{fl/fl}$ T cells in experimental colitis

462 $ST2^{+}$ T_{regs} are protective in intestinal inflammation (Schiering, Krausgruber et al. 2014), in
463 addition they are Th_2 biased and release IL-10 (Siede, Frohlich et al. 2016). To decipher if
464 *Foxp3*^{cre}*CREB*$^{fl/fl}$ T cells prevent colitis by IL-10 production and/or ST2 expression, we
465 performed an adoptive transfer colitis with anti-IL10R antibodies or recombinant soluble ST2
466 (sST2). sST2 acts as a decoy for IL-33 and inhibits its biological activity (Holgado, Braun et
467 al. 2019). Blockade of IL-10 signalling induced a colitis in the formerly resistant
468 *Foxp3*^{cre}*CREB*$^{fl/fl}$ T cell recipient mice (**Fig. 6A-C**), while ST2 blockade had no effect on
469 disease progression (**Supp. Fig. 4**).

470 ## 3.6 Genome-wide chromatin accessibility of WT and CREB-deficient T_{regs}

471 To analyse if CREB deletion alters chromatin accessibility at different promoters and
472 enhancers, we performed the Assay for Transposase-Accessible Chromatin using sequencing
473 (ATAC-seq) in *CREB*$^{fl/fl}$ and *Foxp3*^{cre}*CREB*$^{fl/fl}$ T_{regs}. We observed a decrease in open chromatin
474 around CREB and CREM motifs on *Foxp3*^{cre}*CREB*$^{fl/fl}$ mice, which indicate loss of binding
475 activity of these transcription factors in these cells (**Fig. 7A**). The *Il1rl1* (ST2) region showed
476 significant differences in open chromatin around the promoter and potential enhancer sites in
477 T_{regs} of *Foxp3*^{cre}*CREB*$^{fl/fl}$ mice, while CREB-binding motifs could not be identified (**Fig. 7B**).
478 In addition, the IL-13 enhancer region showed clear differences between the 2 mice strains.
479 Within this region, binding sites for Nrf1 were identified, which is a CREB dependent

480 transcription factor (Suliman, Sweeney et al. 2010). Moreover, we found a change in open
481 chromatin of an alternate promoter of CREM (**Fig. 7B**). CREM has been identified as one of
482 the most regulated genes in ST-2 positive colonic T_{regs} of healthy mice before (Miragaia, Gomes
483 et al. 2019). To prove if CREM is involved in the regulation of ST2 we generated
484 *Foxp3^{cre}CREB$^{fl/fl}$CREM$^{-/-}$* mice. *In vitro* differentiation towards Foxp3+ cells was not
485 significantly diminished in *Foxp3^{cre}CREB$^{fl/fl}$CREM$^{-/-}$* mice (**Fig. 7C**). Furthermore, deletion of
486 CREM normalized Foxp3 expression per cell in CREB-deficient T_{regs} at least to some extent
487 (**Fig. 7D**), however reversed expression of ST2 (**Fig. 7E**). Taken together our data suggest that
488 the interaction of CREB and CREM determine the expression of Foxp3 and ST2 and induction
489 of CREM in CREB deficient T_{regs} contributes to reduced Foxp3 expression. To prove the effect
490 in vivo, we performed a transfer of *Foxp3^{cre}CREB$^{fl/fl}$*CREM$^{-/-}$ T cells (CD4+CD25-) or
491 appropriate wild type T cells (CD4+CD25-) into lymphopenic Rag2$^{-/-}$ mice. The additional
492 genetic deletion of CREM reversed the effect of the CREB deletion and resulted in enhanced
493 colitis severity measured by JLS (The Jackson Laboratory Scoring) score in the transferred mice
494 (**Fig. 7F**).

495

496

497

498

499

500

4 DISCUSSION

In this study we provide evidence that CREB cell-intrinsically regulates Foxp3 expression in T_{regs} and thereby plays a critical role in T_{reg} cell-mediated immune homeostasis. In detail, CREB deficient T_{regs} show a reduced expression of Foxp3 per cell but enhanced expression of ST2, IL-10, and IL-13. Enhanced IL-10 expression of CREB-deficient T_{regs} prevents T cell mediated colitis. Enhanced IL-10 expression is also a hallmark of $ST2^{+}$ T_{regs}. ST2 is expressed on colonic T_{regs} and enhances local intestinal T_{reg} cell responses (Schiering, Krausgruber et al. 2014). We identified particularly enhanced expression of T_{regs} in colon and lung in *Foxp3*^{cre}*CREB*$^{fl/fl}$ mice, which also includes upregulation of ST2 expression, and which might contribute to the unexpectedly protective role of CREB deletion in T_{regs} in type I immune responses. This protective role is in line with Wang et al., who demonstrated an important role for CREB in regulating the balance between Th17 cells and T_{regs} (Wang, Ni et al. 2017). They showed that mice bearing a deletion of CREB in all $CD4^{+}$ T cells prevented T cell mediated transfer colitis comparable to our model. Moreover, these mice were also resistant in an EAE model. This protective effect in EAE was surprisingly lost, when CREB was specifically deleted in T_{regs}. Nevertheless, except from the EAE model Wang et al. did not analyse the Foxp3 specific CREB deleted mice in further detail.

We hypothesize that in particular the enhanced IL-10 secretion prevented colitis in Rag-/- mice transferred with *Foxp3*^{cre}*CREB*$^{fl/fl}$ CD4+ T cells. IL-10 is an important regulator of intestinal homeostasis, as IL10 and IL10R deficient mice spontaneously develop intestinal inflammation (Kuhn, Lohler et al. 1993, Spencer, Di Marco et al. 1998) and blocking IL-10 signalling induced colitis in *Foxp3*^{cre}*CREB*$^{fl/fl}$ T cell recipients that were previously resistant. It has been shown before that CREB induces IL-10 transcription in macrophages. Our data thus were highly unexpected and do not support these findings but might instead argue for cell dependent mechanisms that regulate IL-10 expression. Our ATACseq data however do not show a direct

526 effect of CREB expression on chromatin accessibility within the IL-10 enhancer and promoter
527 region, thus we currently cannot mechanistically explain these findings.
528 We also found enhanced percentages of T_{regs} within the thymus, spleen and pLNs but reduced
529 Foxp3 expression per cell within peripheral lymphoid organs. Wang et al. also suggest that
530 compensation by related transcription factors such as CREM exist. Interestingly and
531 corroborating that theory, we found a clear upregulation of CREM in CREB deficient T_{regs} and
532 additional deletion of CREM recuperates Foxp3 expression in CREB deficient T_{reg} cells, while
533 it downregulates ST2 expression. Strikingly, CREM expression, which was enhanced in
534 *Foxp3^{cre}CREB$^{fl/fl}$* T_{regs} was found before as a highly regulated gene in ST2 positive colon and
535 skin T_{regs} (Miragaia, Gomes et al. 2019). Delacher et al. characterized ST2^{+} tissue T_{regs} that are
536 present in all non-lymphoid tissues, which were found to express killer cell lectin-like receptor
537 subfamily G1 (KLRG1) and Th2 associated factors, including IL-10 (Delacher, Imbusch et al.
538 2017, Delacher, Imbusch et al. 2020). These "tisT_{regs}ST-2" cells are programmed by Basic
539 leucine zipper transcription factor ATF-like (BATF) (Delacher, Imbusch et al. 2020) in
540 lymphoid organs and perform important tissue homeostasis and regenerative functions. Our
541 data point to the fact that the expression of CREB and CREM also regulate these tisT_{reg}ST2 in
542 non-lymphoid tissues like colon, lung and liver. Spath et al. vigorously analysed ST2
543 trajectories in mice and showed a high plasticity in ST2 expression and hierarchies in tissue-
544 specific phenotypes (Spath, Roan et al. 2022). In addition, they found that ST2^{+} T_{regs} were
545 highly proliferative and had a high migratory potential. This goes in line with our findings that
546 these cells can be found in spleen, lung, liver, mLN and the colon. They additionally found a
547 high prevalence in skin and VAT, which was not analysed in our setting. When comparing the
548 transcriptional profiles with our analyses we can confirm an upregulation of PTPN13 in our
549 data (1.97fold) and a regulation of Rab4a (-1.51fold), between the CREB deficient T_{regs} and
550 wild type T_{regs}, the other factors that distinguished ST2^{+} from ST2^{-} T_{regs} (Lyn, Gata3, Rln3,
551 Klrg1, and Tbc1d4) were not different. Interestingly, in their analysis, ST2^{+} T_{regs} were enriched

552 in more activated, differentiated T_{reg} populations such as $ID2^+$ T_{regs} and ID2 was upregulated in
553 our analysis as well (1.7fold) (Spath, Roan et al. 2022).
554 Limitations of our study are that we mechanistically mainly analysed splenic T_{regs}, while ST2
555 is a hallmark of tissue T_{regs} and further analysis will show how this will affect local T_{regs} and
556 tissue homeostasis. Another issue is that it is not clear how CREB activation is regulated in
557 T_{regs}. CREB has nine serine residues in the kinase inducible domain (KID) that can be
558 phosphorylated and activated by different kinases and different phosphorylation patterns of
559 CREB can exert opposite effects. Further research will therefore also be necessary to identify
560 therapeutic targets to directly influence CREB activity in T_{regs}. In conclusion, we provide
561 evidence that CREB plays a pivotal role in T_{regs}. CREB is an important transcription factor to
562 maintain Foxp3 expression and the interaction of CREM and CREB are crucial for the
563 expression of ST2 in T_{regs}. A lack of CREB enhances IL-10 expression and thereby prevents
564 Th1 mediated diseases.

565 AUTHOR CONTRIBUTIONS

566 S.H.S conducted the experiments, analysed the data and wrote the manuscript. J.H, S.S, T.L,
567 T.G, C.N, T.C, M.S, E.V, S.B, K.O & S.F conducted experiments, M.K contributed to study
568 design, K.O, I.C, Z.L, L.G, B.D, & S.F analysed data, J.H & M.Z analysed data and contributed
569 to study design, E.S, R.B, & B.L provided reagents, A.S provided the mice, T.B provided mice
570 and contributed to study design, N.W contributed to reviewing the manuscript, K.O & K.T
571 revised the manuscript and designed the study.
572

573 DECLARATION OF COMPETING INTEREST

574 The authors declare that they have no known competing financial interests or personal
575 relationships that could have appeared to influence the work reported in this paper.

ACKNOWLEDGMENTS

This research project was supported by DFG grant TE339/20-1 to K.T. J.H and T.B were supported by the DFG grant SFB/TRR 355/1 (Project number: 490846870). The authors acknowledge the IZKF Flow Cytometry Facility for the use of cell sorter (DFG grant project ID 439895892) and Genomics facility for their service.

596 ## REFERENCES

597 Asahara, H., et al. (2001). "Chromatin-dependent cooperativity between constitutive and inducible
598 activation domains in CREB." Mol Cell Biol **21**(23): 7892-7900.

599
600 Baron, U., et al. (2007). "DNA demethylation in the human FOXP3 locus discriminates regulatory T
601 cells from activated FOXP3(+) conventional T cells." Eur J Immunol **37**(9): 2378-2389.

602
603 Barton, K., et al. (1996). "Defective thymocyte proliferation and IL-2 production in transgenic mice
604 expressing a dominant-negative form of CREB." Nature **379**(6560): 81-85.

605
606 Bennett, C. L., et al. (2001). "The immune dysregulation, polyendocrinopathy, enteropathy, X-linked
607 syndrome (IPEX) is caused by mutations of FOXP3." Nat Genet **27**(1): 20-21.

608
609 Bleich, A., et al. (2004). "Refined histopathologic scoring system improves power to detect colitis QTL
610 in mice." Mamm Genome **15**(11): 865-871.

611
612 Bodor, J., et al. (2012). "Cyclic AMP underpins suppression by regulatory T cells." Eur J Immunol
613 **42**(6): 1375-1384.

614
615 Bopp, T., et al. (2007). "Cyclic adenosine monophosphate is a key component of regulatory T cell-
616 mediated suppression." J Exp Med **204**(6): 1303-1310.

617
618 Brenner, S., et al. (2003). "cAMP-induced Interleukin-10 promoter activation depends on
619 CCAAT/enhancer-binding protein expression and monocytic differentiation." J Biol Chem **278**(8):
620 5597-5604.

621
622 Corces, M. R., et al. (2017). "An improved ATAC-seq protocol reduces background and enables
623 interrogation of frozen tissues." Nat Methods **14**(10): 959-962.

624
625 De Cesare, D. and P. Sassone-Corsi (2000). "Transcriptional regulation by cyclic AMP-responsive
626 factors." Prog Nucleic Acid Res Mol Biol **64**: 343-369.

627
628 Delacher, M., et al. (2020). "Precursors for Nonlymphoid-Tissue Treg Cells Reside in Secondary
629 Lymphoid Organs and Are Programmed by the Transcription Factor BATF." Immunity **52**(2): 295-312
630 e211.

631
632 Delacher, M., et al. (2017). "Genome-wide DNA-methylation landscape defines specialization of
633 regulatory T cells in tissues." Nat Immunol **18**(10): 1160-1172.

634
635 Dorsey, M. J., et al. (1995). "B-ATF: a novel human bZIP protein that associates with members of the
636 AP-1 transcription factor family." Oncogene **11**(11): 2255-2265.

637
638 Drake, L. Y. and H. Kita (2017). "IL-33: biological properties, functions, and roles in airway disease."
639 Immunol Rev **278**(1): 173-184.

640
641 Floess, S., et al. (2007). "Epigenetic control of the foxp3 locus in regulatory T cells." PLoS Biol **5**(2):
642 e38.

643
644 Foulkes, N. S., et al. (1991). "CREM gene: use of alternative DNA-binding domains generates multiple
645 antagonists of cAMP-induced transcription." Cell **64**(4): 739-749.

646
647 Garg, G., et al. (2019). "Blimp1 Prevents Methylation of Foxp3 and Loss of Regulatory T Cell Identity
648 at Sites of Inflammation." Cell Rep **26**(7): 1854-1868 e1855.

649
650 Griesenauer, B. and S. Paczesny (2017). "The ST2/IL-33 Axis in Immune Cells during Inflammatory
651 Diseases." Front Immunol. **24;8:475.**

652
653 Hedrich, C. M., et al. (2011). "cAMP-responsive element modulator (CREM)alpha protein signaling
654 mediates epigenetic remodeling of the human interleukin-2 gene: implications in systemic lupus
655 erythematosus." J Biol Chem **286**(50): 43429-43436.

656
657 Holgado, A., et al. (2019). "IL-33trap is a novel IL-33-neutralizing biologic that inhibits allergic airway
658 inflammation." J Allergy Clin Immunol **144**(1): 204-215.

659
660 Irizarry, R. A., et al. (2003). "Exploration, normalization, and summaries of high density
661 oligonucleotide array probe level data." Biostatistics **4**(2): 249-264.

662
663 Kakkar, R. and R. Lee (2008). "The IL-33/ST2 pathway: therapeutic target and novel biomarker." Nat
664 Rev Drug Discov.: 7(10):827-840.

665
666 Kim, H. P. and W. J. Leonard (2007). "CREB/ATF-dependent T cell receptor-induced FoxP3 gene
667 expression: a role for DNA methylation." J Exp Med **204**(7): 1543-1551.

668
669 Kuhn, R., et al. (1993). "Interleukin-10-deficient mice develop chronic enterocolitis." Cell **75**(2): 263-
670 274.

671
672 Lal, G. and J. S. Bromberg (2009). "Epigenetic mechanisms of regulation of Foxp3 expression." Blood
673 **114**(18): 3727-3735.

674
675 Langmead, B. and S. L. Salzberg (2012). "Fast gapped-read alignment with Bowtie 2." Nat Methods
676 **9**(4): 357-359.

677
678 Li, H., et al. (2009). "The Sequence Alignment/Map format and SAMtools." Bioinformatics **25**(16):
679 2078-2079.

680
681 Li, Z., et al. (2019). "Identification of transcription factor binding sites using ATAC-seq." Genome Biol
682 **20**(1): 45.

683
684 Liao, W., et al. (2011). "IL-2 family cytokines: new insights into the complex roles of IL-2 as a broad
685 regulator of T helper cell differentiation." Curr Opin Immunol **23**(5): 598-604.

686
687 Lippe, R., et al. (2012). "CREMalpha overexpression decreases IL-2 production, induces a T(H)17
688 phenotype and accelerates autoimmunity." J Mol Cell Biol **4**(2): 121-123.

689
690 Manna, P. R. and D. M. Stocco (2007). "Crosstalk of CREB and Fos/Jun on a single cis-element:
691 transcriptional repression of the steroidogenic acute regulatory protein gene." J Mol Endocrinol
692 **39**(4): 261-277.

693
694 Miragaia, R. J., et al. (2019). "Single-Cell Transcriptomics of Regulatory T Cells Reveals Trajectories of
695 Tissue Adaptation." Immunity **50**(2): 493-504 e497.

696
697 Murai, M., et al. (2009). "Interleukin 10 acts on regulatory T cells to maintain expression of the
698 transcription factor Foxp3 and suppressive function in mice with colitis." Nat Immunol **10**(11): 1178-
699 1184.

700
701 Ohl, K. and K. Tenbrock (2015). "Regulatory T cells in systemic lupus erythematosus." Eur J Immunol
702 **45**(2): 344-355.

703
704 Ohl, K., et al. (2015). "IL-2 treatment reverses effects of CREMalpha-overexpressing T cells in
705 autoimmune-prone mice." Clin Exp Immunol.

706
707 Okamoto, A., et al. (2011). "Regulatory T-cell-associated cytokines in systemic lupus erythematosus."
708 J Biomed Biotechnol **2011**: 463412.

709
710 Okawa, H., et al. (2006). "Hepatocyte-specific deletion of the keap1 gene activates Nrf2 and confers
711 potent resistance against acute drug toxicity." Biochem Biophys Res Commun **339**(1): 79-88.

712
713 Pils, M. C., et al. (2011). "Commensal gut flora reduces susceptibility to experimentally induced colitis
714 via T-cell-derived interleukin-10." Inflamm Bowel Dis **17**(10): 2038-2046.

715
716 Polansky, J. K., et al. (2010). "Methylation matters: binding of Ets-1 to the demethylated Foxp3 gene
717 contributes to the stabilization of Foxp3 expression in regulatory T cells." J Mol Med (Berl) **88**(10):
718 1029-1040.

719
720 Powell, J. D., et al. (1999). "The -180 site of the IL-2 promoter is the target of CREB/CREM binding in T
721 cell anergy." J Immunol **163**(12): 6631-6639.

722

723 Rauen, T., et al. (2011). "cAMP-responsive Element Modulator (CREM)α Protein Induces Interleukin
724 17A Expression and Mediates Epigenetic Alterations at the Interleukin-17A Gene Locus in Patients
725 with Systemic Lupus Erythematosus." Journal of Biological Chemistry **286**(50): 43437-43446.

726
727 Ruan, Q., et al. (2009). "Development of Foxp3(+) regulatory t cells is driven by the c-Rel
728 enhanceosome." Immunity **31**(6): 932-940.

729
730 Rubtsov, Y. P., et al. (2008). "Regulatory T cell-derived interleukin-10 limits inflammation at
731 environmental interfaces." Immunity **28**(4): 546-558.

732
733 Sanin, D. E., et al. (2015). "IL-10 Production in Macrophages Is Regulated by a TLR-Driven CREB-
734 Mediated Mechanism That Is Linked to Genes Involved in Cell Metabolism." J Immunol **195**(3): 1218-
735 1232.

736
737 Sassone-Corsi, P. (1995). "Transcription factors responsive to cAMP." Annu Rev Cell Dev Biol **11**: 355-
738 377.

739
740 Schiering, C., et al. (2014). "The alarmin IL-33 promotes regulatory T-cell function in the intestine."
741 Nature **513**(7519): 564-568.

742
743 Setoguchi, R., et al. (2005). "Homeostatic maintenance of natural Foxp3(+) CD25(+) CD4(+) regulatory
744 T cells by interleukin (IL)-2 and induction of autoimmune disease by IL-2 neutralization." J Exp Med
745 **201**(5): 723-735.

746
747 Siede, J., et al. (2016). "IL-33 Receptor-Expressing Regulatory T Cells Are Highly Activated, Th2 Biased
748 and Suppress CD4 T Cell Proliferation through IL-10 and TGFbeta Release." PLoS One **11**(8):
749 e0161507.

750
751 Solomou, E. E., et al. (2001). "Molecular basis of deficient IL-2 production in T cells from patients with
752 systemic lupus erythematosus." J Immunol **166**(6): 4216-4222.

753
754 Spath, S., et al. (2022). "Profiling of Tregs across tissues reveals plasticity in ST2 expression and
755 hierarchies in tissue-specific phenotypes." iScience **25**(9): 104998.

756
757 Spencer, S. D., et al. (1998). "The orphan receptor CRF2-4 is an essential subunit of the interleukin 10
758 receptor." J Exp Med **187**(4): 571-578.

759
760 Suliman, H. B., et al. (2010). "Co-regulation of nuclear respiratory factor-1 by NFkappaB and CREB
761 links LPS-induced inflammation to mitochondrial biogenesis." J Cell Sci **123**(Pt 15): 2565-2575.

762
763 Tenbrock, K., et al. (2006). "The transcriptional repressor cAMP response element modulator alpha
764 interacts with histone deacetylase 1 to repress promoter activity." J Immunol **177**(9): 6159-6164.

765

766 Thornton, A. M., et al. (2019). "Helios(+) and Helios(-) Treg subpopulations are phenotypically and
767 functionally distinct and express dissimilar TCR repertoires." Eur J Immunol **49**(3): 398-412.

768

769 Tsuji, M., et al. (2009). "Preferential generation of follicular B helper T cells from Foxp3+ T cells in gut
770 Peyer's patches." Science **323**(5920): 1488-1492.

771

772 Unutmaz, D. and B. Pulendran (2009). "The gut feeling of Treg cells: IL-10 is the silver lining during
773 colitis." Nat Immunol **10**(11): 1141-1143.

774

775 Via, C. S., et al. (1993). "T cell-antigen-presenting cell interactions in human systemic lupus
776 erythematosus. Evidence for heterogeneous expression of multiple defects." J Immunol **151**(7):
777 3914-3922.

778

779 Wang, J., et al. (2013). "WEB-based GEne SeT AnaLysis Toolkit (WebGestalt): update 2013." Nucleic
780 Acids Res **41**(Web Server issue): W77-83.

781

782 Wang, X., et al. (2017). "Cyclic AMP-Responsive Element-Binding Protein (CREB) is Critical in
783 Autoimmunity by Promoting Th17 but Inhibiting Treg Cell Differentiation." EBioMedicine **25**: 165-
784 174.

785

786 Wang, Y., et al. (2010). "An intrinsic mechanism predisposes Foxp3-expressing regulatory T cells to
787 Th2 conversion in vivo." J Immunol **185**(10): 5983-5992.

788

789 Wildin, R. S., et al. (2001). "X-linked neonatal diabetes mellitus, enteropathy and endocrinopathy
790 syndrome is the human equivalent of mouse scurfy." Nat Genet **27**(1): 18-20.

791

792 Yoshida, N., et al. (2016). "ICER is requisite for Th17 differentiation." Nat Commun. **7: 12993.**

793

794 Zhang, Y., et al. (2008). "Model-based analysis of ChIP-Seq (MACS)." Genome Biol **9**(9): R137.

795

796 Zheng, Y., et al. (2010). "Role of conserved non-coding DNA elements in the Foxp3 gene in regulatory
797 T-cell fate." Nature **463**(7282): 808-812.

798

799 Zhou, X., et al. (2009). "Instability of the transcription factor Foxp3 leads to the generation of
800 pathogenic memory T cells in vivo." Nat Immunol **10**(9): 1000-1007.

801

802 Zorn, E., et al. (2006). "IL-2 regulates FOXP3 expression in human CD4+CD25+ regulatory T cells
803 through a STAT-dependent mechanism and induces the expansion of these cells in vivo." Blood
804 **108**(5): 1571-1579.

805

806

± SEM.

APPENDIX A

FIGURES

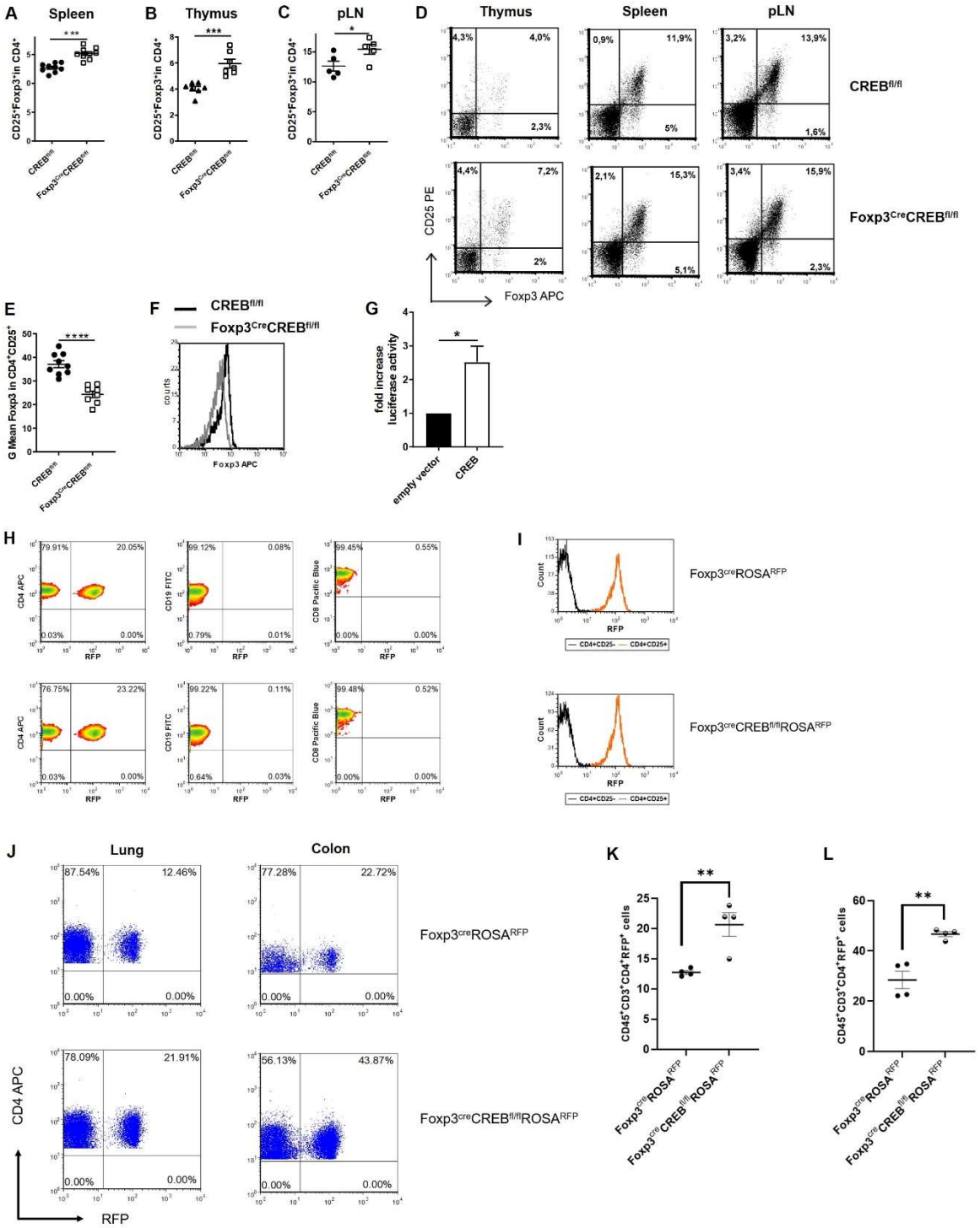

Figure 1: Genetic deletion of CREB in Foxp3$^+$ cells enhance percentages of T_{regs} but downregulates their Foxp3 expression. A) Statistical analysis of splenic T_{reg} ($CD4^+CD25^+Foxp3^+$) percentages from *CREB$^{fl/fl}$* and *Foxp3^{cre}CREB$^{fl/fl}$* mice (N = 9, 4 independently performed experiments, each with 2-3 age

814 and sex-matched mice, 6-9 weeks old). **B)** Statistical analysis of T_{reg} percentages within thymus
815 ($CD3^+CD4^{sp}CD25^+Foxp3^+$) from *CREB*$^{fl/fl}$ and *Foxp3*^{cre}*CREB*$^{fl/fl}$ mice (*N* = 7, 3 independently performed
816 experiments, each with 2-3 age and sex-matched mice, 6-9 weeks old). **C)** Statistical analysis of T_{reg}
817 ($CD4^+CD25^+Foxp3^+$) percentages from pLNs from *CREB*$^{fl/fl}$ and *Foxp3*^{CRE}*CREB*$^{fl/fl}$ (*N* =5, 2
818 independently performed experiments, each with 2-3 age and sex-matched mice 7-9 weeks old). **D)**
819 Density plot showing $CD25^+Foxp3^+$ cells gated on $CD3^+CD4^+CD8^-$ cells in thymus of *CREB*$^{fl/fl}$ and
820 *Foxp3*^{cre}*CREB*$^{fl/fl}$ mice (left), $CD25^+Foxp3^+$ cells gated on $CD4^+$ cells in spleens of *CREB*$^{fl/fl}$ and
821 *Foxp3*^{cre}*CREB*$^{fl/fl}$ mice (middle) and $CD4^+CD25^+$Foxp3+ cells in pLN of *CREB*$^{fl/fl}$ and *Foxp3*^{cre}*CREB*$^{fl/fl}$
822 mice (right). **E**) Statistical analysis of mean fluorescent intensity (MFI) of Foxp3 in *CREB*$^{fl/fl}$ and
823 *Foxp3*^{cre}*CREB*$^{fl/fl}$ $CD4^+CD25^+$ T cells (*N=6*, 3 independently performed experiments, each with 2
824 animals, 6-8 weeks old, sex and age matched). **F**) Representative histogram showing overlay of Foxp3
825 expression in $CD4^+CD25^+$ cells from *CREB*$^{fl/fl}$(black) and *Foxp3*^{cre}*CREB*$^{fl/fl}$ (grey) spleens. **G)** RLM
826 cells carrying a stable pGL3-TSDR-FoxPro luciferase Plasmid were transfected either with an empty
827 vector or CREB plasmid, stimulated with PMA and luciferase activity was measured after 4 hours (*N* =
828 *5*). **H)** Percentages of RFP^+ cells within the $CD4^+$ (on the left), $CD19^+$ (in the middle) and $CD8^+$
829 population (on the right) in spleens of *Foxp3*^{cre}*ROSA*^{RFP} and *Foxp3*^{cre}*CREB*$^{fl/fl}$*ROSA*^{RFP} mice. **I)**
830 Representative histogram showing MFI of RFP expression in $CD4^+$CD25- (black) and $CD4^+CD25^+$ cells
831 (red) in spleens of *Foxp3*^{cre}*ROSA*^{RFP} *and Foxp3*^{cre}*CREB*$^{fl/fl}$*ROSA*^{RFP} mice. **J)** Percentages of RFP^+ cells
832 within the $CD45^+CD3^+CD4^+$ population in lung and colon of *Foxp3*^{cre}*ROSA*^{RFP} and
833 *Foxp3*^{cre}*CREB*$^{fl/fl}$*ROSA*^{RFP} mice. **K)** Statistical analysis of $CD45^+CD3^+CD4^+RFP^+$ cells in lung tissue of
834 *Foxp3*^{CRE}*ROSA*^{RFP} *and Foxp3*^{cre}*CREB*$^{fl/fl}$*ROSA*^{RFP} mice (*N=4*, three independently performed
835 experiments) **L)** Statistical analysis of $CD45^+CD3^+CD4^+RFP^+$ cells in colon tissue of *Foxp3*^{cre}*ROSA*^{RFP}
836 and *Foxp3*^{cre}*CREB*$^{fl/fl}$*ROSA*^{RFP} mice (*N=4*, three independently performed experiments). A two-tailed,
837 unpaired t-tests was used to test significance. *p<0.05, **p<0.01, ***p<0.001, ****p<0.0001 and
838 results are expressed as the mean ± SEM.
839
840

841

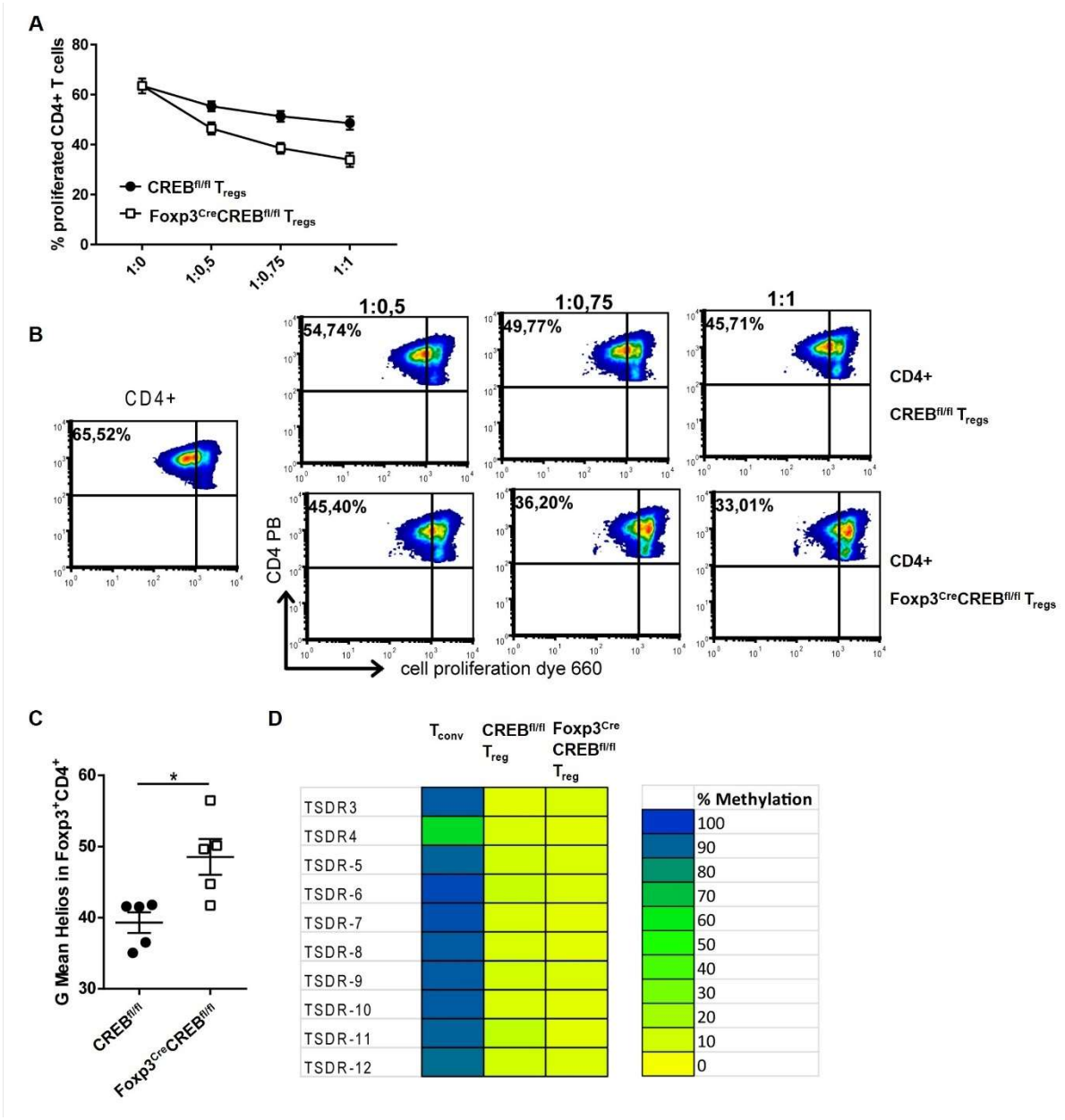

842

843 **Figure 2: *In vitro* suppressive capacity of T_{regs} is enhanced in the absence of CREB. A)** WT $CD4^+$
844 T cells from spleens (T_{eff}) were labeled with efluor660 and stimulated with anti-CD3/CD28 antibodies.
845 $CD4^+CD25^+$ T cells (T_{regs}) from *CREB*$^{fl/fl}$ or *Foxp3*^{cre}*CREB*$^{fl/fl}$ animals were added in different ratios.
846 The proliferation of responder T cells was assessed by efluor660 (ebioscience) dilution (*N = 3*) **B)**
847 Representative density plots of A). **C)** Statistical analysis of MFI of Helios in *CREB*$^{fl/fl}$ and
848 Foxp*3*^{cre}*CREB*$^{fl/fl}$ $CD4^+Foxp3^+$ T cells (*N = 5*, 2 independently performed experiments, each with 2-3
849 animals, 8 weeks old sex-matched, a two-tailed Mann Whitney test was performed to test for
850 significance). **D)** Representative TSDR methylation patterns of purified $CD4^+CD25^+Nrp1^+$ T_{reg} cells
851 and $CD4^+CD25^-$ conventional T cells isolated from spleens of 6-8 weeks old male mice (*N = 4*).
852 Amplicons are vertically arranged, each representing a single CpG-motif. The methylation rate of each
853 motif was translated into a yellow-green-blue color code. *$p<0.05$ and all results are expressed as the
854 mean ± SEM.

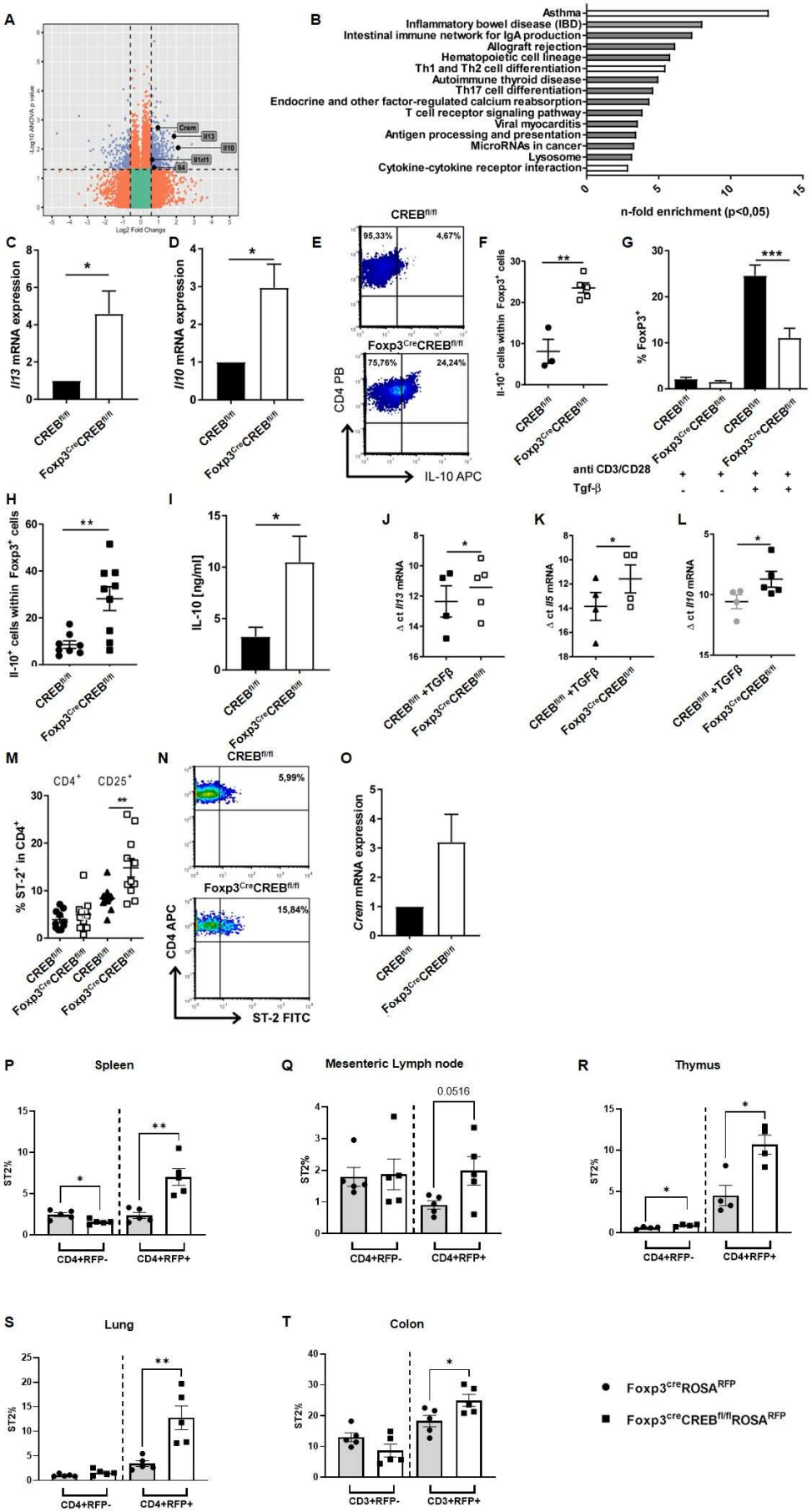
A
Crem
Il13
Il10
Il1rl1
Il5
Log2 Fold Change
B
Asthma
Inflammatory bowel disease (IBD)
Intestinal immune network for IgA production
Allograft rejection
Hematopoietic cell lineage
Th1 and Th2 cell differentiation
Autoimmune thyroid disease
Th17 cell differentiation
Endocrine and other factor-regulated calcium reabsorption
T cell receptor signaling pathway
Viral myocarditis
Antigen processing and presentation
MicroRNAs in cancer
Lysosome
Cytokine-cytokine receptor interaction
n-fold enrichment (p<0,05)
C
Il13 mRNA expression
D
Il10 mRNA expression
E
CREBfl/fl
95,33%
4,67%
Foxp3CreCREBfl/fl
75,76%
24,24%
CD4 PB
IL-10 APC
F
Il-10+ cells within Foxp3+ cells
G
% FoxP3+
anti CD3/CD28
Tgf-β
H
Il-10+ cells within Foxp3+ cells
I
IL-10 [ng/ml]
J
Δ ct Il13 mRNA
K
Δ ct Il5 mRNA
L
Δ ct Il10 mRNA
M
CD4+
CD25+
% ST-2+ in CD4+
N
CREBfl/fl
5,99%
Foxp3CreCREBfl/fl
15,84%
CD4 APC
ST-2 FITC
O
Crem mRNA expression
P
Spleen
ST2%
CD4+RFP-
CD4+RFP+
Q
Mesenteric Lymph node
0.0516
R
Thymus
S
Lung
T
Colon
CD3+RFP-
CD3+RFP+
Foxp3creROSARFP
Foxp3creCREBfl/flROSARFP

855

856 **Figure 3: Altered gene expression in CREB deficient T_{regs}. A)** Gene expression in T_{regs} from spleens
857 of *CREB*$^{fl/fl}$ and *Foxp3*^{cre}*CREB*$^{fl/fl}$ *mice.* Colors indicate significant upregulation or downregulation of at
858 least 1.5-fold with p-value not more than 0.05 (blue); regulation of at least 1.5-fold or regulation with
859 p-value not more than 0.05 (red). **B)** Selection of pathways and associated genes, which were
860 significantly enriched. **C)** N-fold *Il13* mRNA expression in splenic T_{regs} from from *CREB*$^{fl/fl}$ and
861 *Foxp3*^{cre}*CREB*$^{fl/fl}$ mice (*N = 5*, male, 8-10 weeks old) analyzed by RT-qPCR. Bars indicate mean and
862 error bars SEM, two-tailed one-sample test. **D)** N-fold *Il10* mRNA expression in splenic T_{regs} from
863 *CREB*$^{fl/fl}$ and *Foxp3*^{cre}*CREB*$^{fl/fl}$ mice (*N = 5*, male, 8-10 weeks old) analyzed by RT-qPCR. Bars indicate
864 mean and error bars SEM, two-tailed one sample test. **E)** MACS-isolated T cells from spleens were
865 stimulated ex-vivo with anti-CD3/CD28 antibodies for three days and re-stimulated with
866 PMA/Ionomycin in the presence of Golgi Plug™. A representative density plot shows IL-10 production
867 in $CD4^+Foxp3^+$ cells **F)** Statistical analysis of IL-10 expression of $Foxp3^+$ cells after treatment as in E)
868 (*N = 3* independent experiments, each dot represents one animal, two tailed unpaired t-test. **G)**
869 $CD4^+CD25^-$ T cells were stimulated with anti-CD3/CD28 antibodies in the presence/absence of 5 ng/ml
870 TGF-β for five days. Percentages of $Foxp3^+$ cells from 6 independently performed experiments were
871 determined, each with spleen from one mouse (*N =13 CREB*$^{fl/fl}$ and *N=12 Foxp3*^{cre}*CREB*$^{fl/fl}$ mice), a two
872 tailed unpaired t-test was used to test for significance. **H)** Statistical analysis of IL-10^+ cells within
873 $Foxp3^+$ cells after treatment as in G). An unpaired, two tailed t-test was used to test for significance,
874 each dot represents one animal and error bars SEM **I)** IL-10 in supernatants of $CD4^+CD25^-$ T cells after
875 stimulation with anti-CD3/CD28 antibodies in the presence of 5 ng/ml TGF-β for five days measured
876 by ELISA, an unpaired two- tailed t test was performed to test for significance, bars indicate mean and
877 error bars SEM (*N = 6*). **J)-L)** Δ ct mRNA expression of cells after treatment as in G, each dot represents
878 one animal and error bars SEM, two tailed unpaired t-tests were used to test for significance. **M)**
879 Statistical analysis of splenic $ST2^+$ cells within $CD4^+$ and $CD4^+CD25^+$ cells of *CREB*$^{fl/fl}$ and
880 *Foxp3*^{cre}*CREB*$^{fl/fl}$ mice. 3 independently performed experiments (*N = 10 CREB*$^{fl/fl}$ and *N =11*
881 *Foxp3*^{cre}*CREB*$^{fl/fl}$ mice), a two tailed unpaired t-test was used to test for significance, each dot represents
882 one animal and error bars SEM. **N)** Representative density plot of M. **O)** N-fold *Crem* mRNA expression

883 in splenic T_{regs} from from *CREB*$^{fl/fl}$ and *Foxp3*^{cre}*CREB*$^{fl/fl}$ mice (N = 3, male, 8-10 weeks old) cells
884 analyzed by RT-qPCR. **P-T)** Statistical analysis of ST2^{+} in CD4+ and CD4+RFP+ cells in
885 *Foxp3*^{cre}*ROSA*^{RFP} (*N = 5*) and *Foxp3*^{cre}*CREB*$^{fl/fl}$*ROSA*^{RFP} (N = 5) in **P)** spleen, **Q)** mesenteric
886 lymph node, **R)** thymus, **S)** lung, bars indicate mean and error bars SEM, two tailed unpaired
887 t-test was used to test for significance. **T)** Statistical analysis of ST2+ in CD3+ and CD3+RFP+
888 cells in *Foxp3*^{cre}*ROSA*^{RFP} (*N = 5*) and *Foxp3*^{cre}*CREB*$^{fl/fl}$*ROSA*^{RFP} (*N = 5*) in colon, two tailed
889 unpaired t-test was used to test for significance. *p<0.05, **p<0.01, ***p<0.001, and results are
890 expressed as the mean ± SEM.

891

892

893

894

895

896

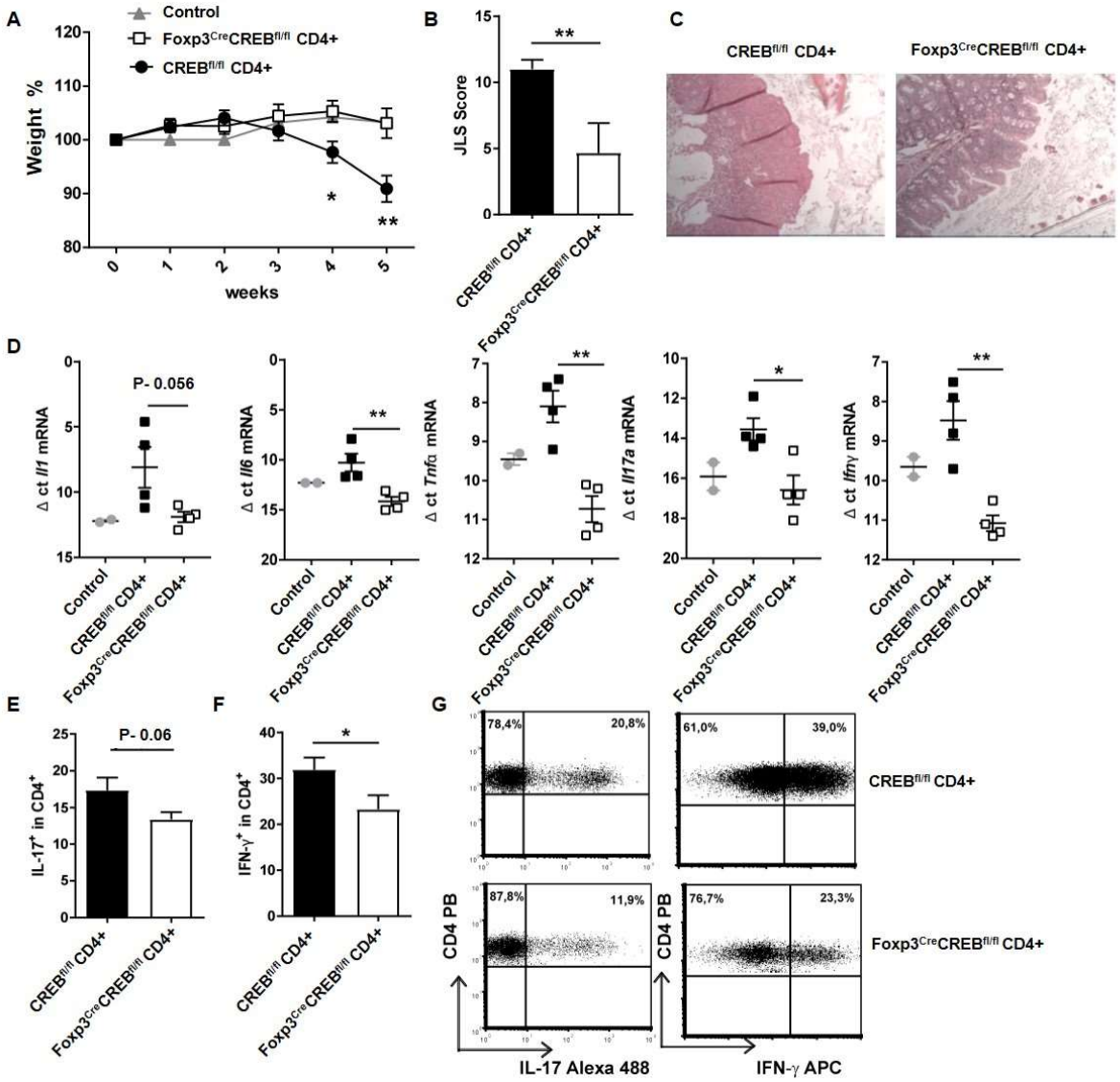

Figure 4: *Foxp3^{cre}CREB$^{fl/fl}$* CD4+ T cells induce only moderate inflammation in experimental colitis. Rag2$^{-/-}$ mice were adoptively transferred with CD4^{+} CD25^{-} wild-type cells (*CREB$^{fl/fl}$* CD4^{+}) or *Foxp3^{cre}CREB$^{fl/fl}$* CD4^{+} CD25^{-} T cells. Untreated Rag$^{-/-}$ mice were used as controls. Mice were weighed and sacrificed 5 weeks after transfer. **A)** Body weight as a percent of starting weight, two-tailed unpaired t-test were used to test for significance (*N = 11 CREB$^{fl/fl}$*, *N = 9 Foxp3^{cre}CREB$^{fl/fl}$* recipients and *5* control Rag$^{-/-}$ mice were analyzed in 3 independently performed experiments). **B)** Results of histological JLS (The Jackson Laboratory Scoring) score of colon sections (two independently performed experiments, *CREB$^{fl/fl}$* recipients N = 5, *Foxp3^{cre}CREB$_{fl/fl}$* recipients N = 6, a two-tailed Mann Whitney test was used). **C)** Representative photomicrographs of hematoxylin and eosin (H&E)-stained colon sections imaged using a 10x objective. **D)** Expression of inflammatory cytokines analyzed by RT-qPCR. Dots represent Δ ct values normalized to β-actin. Each dot represents one animal. (ct levels are inversely proportional to the amount of target nucleic acid in the sample), two tailed unpaired t-tests were used to test for significance, each dot represents one animal (*N = 2* control mice, *N = 4 CREB$^{fl/f}$*, *N = 4 Foxp3^{cre}CREB$^{fl/fl}$*

912 recipients). **E)** Statistical analysis of IL-17^{+} cells within CD4^{+} cells in mLNs (three independently
913 performed experiments, *CREB*$^{fl/fl}$ recipients N = 9, *Foxp3*^{cre}*CREB*$^{fl/fl}$ recipients N = 9), a two-tailed,
914 unpaired t-test was used. **F)** Statistical analysis of IFN-γ^{+} cells within CD4^{+} cells in mLNs. (three
915 independently performed experiments, *CREB*$^{fl/fl}$ recipients *N = 11*, *Foxp3*^{cre}*CREB*$^{fl/fl}$ recipients *N = 9*),
916 two-tailed, unpaired t-test was used. **G)** Representative dot plots of E and F. *$p<0.05$, **$p<0.01$ and
917 results are expressed as the mean ± SEM.

918

919

920

921

922

923

924

925

926

927

928

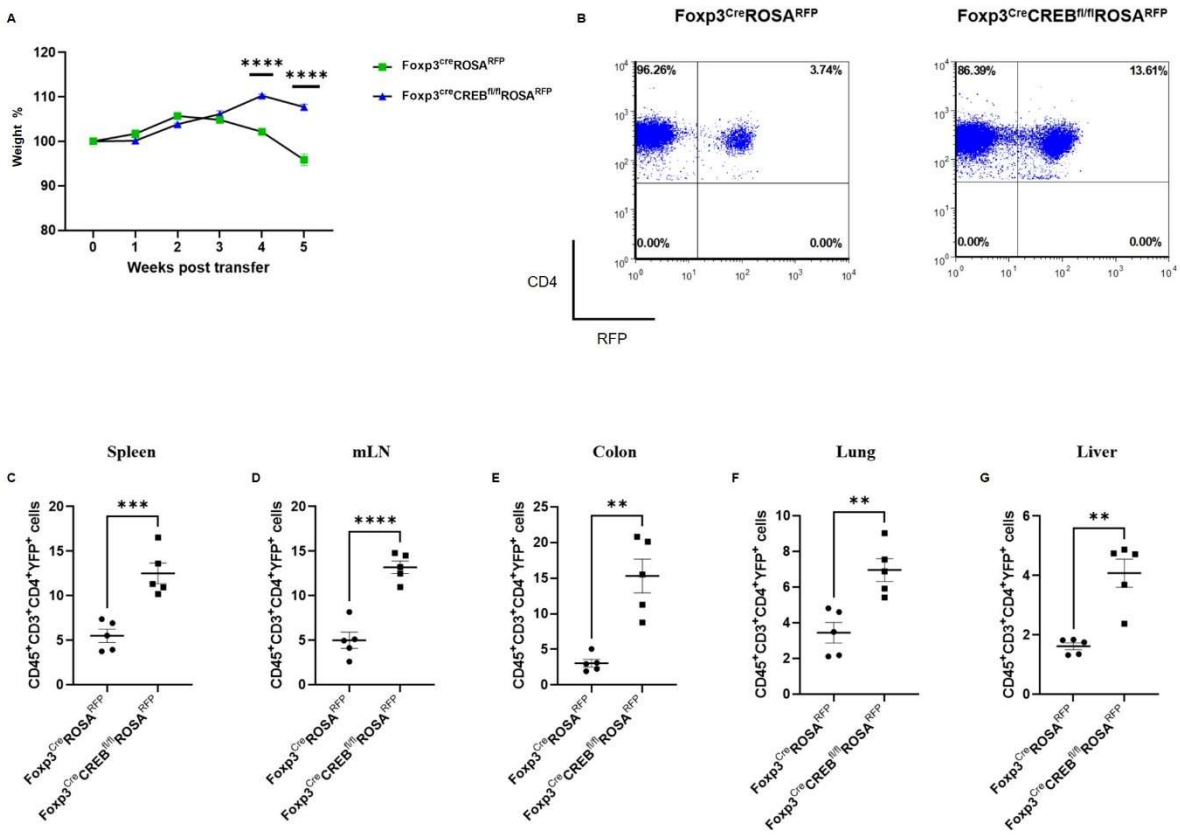

929

930

931 **Figure 5: *Foxp3^{cre}CREB$^{fl/fl}$ROSA^{RFP}* CD4+ T cells induce only moderate inflammation in**
932 **experimental colitis, while CD4+RFP+ cells expand in peripheral tissues.** Rag2$^{-/-}$ mice were
933 adoptively transferred with CD4^{+} CD25^{-} wild-type cells (*Foxp^{cre}ROSA^{RFP}*CD4^{+}) or
934 *Foxp3^{cre}CREB$^{fl/lf}$ROSA^{RFP}* CD4^{+} CD25^{-} T cells. Mice were weighed and sacrificed 5 weeks after
935 transfer. **A)** Body weight as a percent of starting weight, two-tailed unpaired t-test were used to test for
936 significance (*N = 5 Foxp^{cre}ROSA^{RFP}* and *N = 5 Foxp3^{cre}CREB$^{fl/lf}$ROSA^{RFP}* recipient mice were analyzed
937 in 1 independently performed experiment). **B)** Representative Flow cytometry gated on CD4 and RFP
938 in splenocytes. Percentages of CD45^{+}CD3^{+}CD4^{+}RFP^{+} cells in **C)** Spleen, **D)** mLNs, **E)** Colon, **F)** Lung,
939 and **G)** Liver, two-tailed, unpaired t-test was used. **p<0.01, ***p<0.001, ****p<0.0001 and results
940 are expressed as the mean ± SEM.

941

942

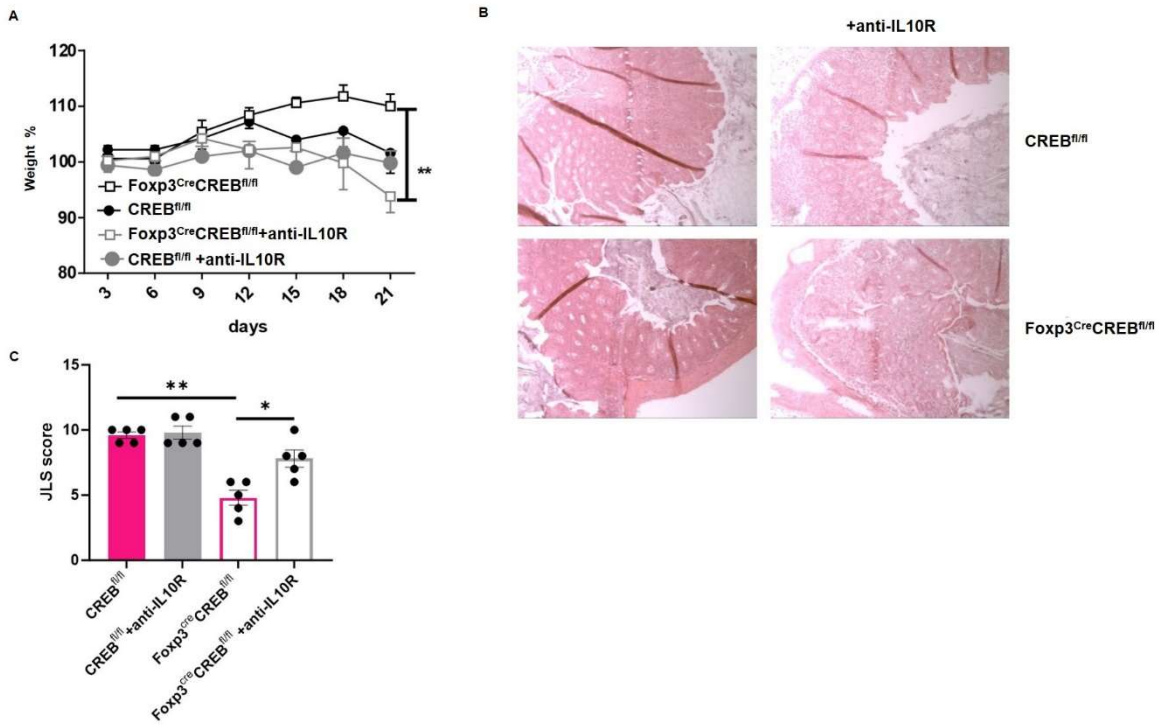

Figure 6: Reduced colitis in *Foxp3^{cre}CREB$^{fl/fl}$* CD4^{+} T cell recipients depends on IL-10 signaling. Rag2$^{-/-}$ mice were adoptively transferred with CD4^{+} wild-type cells (WT CD4^{+}) or *Foxp3^{cre}CREB$^{fl/fl}$* CD4^{+} T cells. Mice were either treated with an anti-IL10R antibody or an isotype control. **A)** Body weight as a percent of starting weight, Bars indicate mean and error bars SEM (*N=5* animals in each group, a two-tailed unpaired t-test was used, two independently performed experiments). **B)** Representative photomicrographs of a hematoxylin and eosin (H&E)-stained colon section from *CREB$^{fl/fl}$* and *Foxp3^{cre}CREB$^{fl/fl}$* CD4^{+} T cell recipients, that were treated with anti-IL10R, imaged using a 10x objective. **C)** Results of histological JLS (The Jackson Laboratory Scoring) score of colon sections (two independently performed experiments with overall *N=5* mice in each group, two-independently performed experiments, a two tailed Mann Whitney test was used to test for significance). *$p<0.05$, **$p<0.01$ and results are expressed as the mean ± SEM.

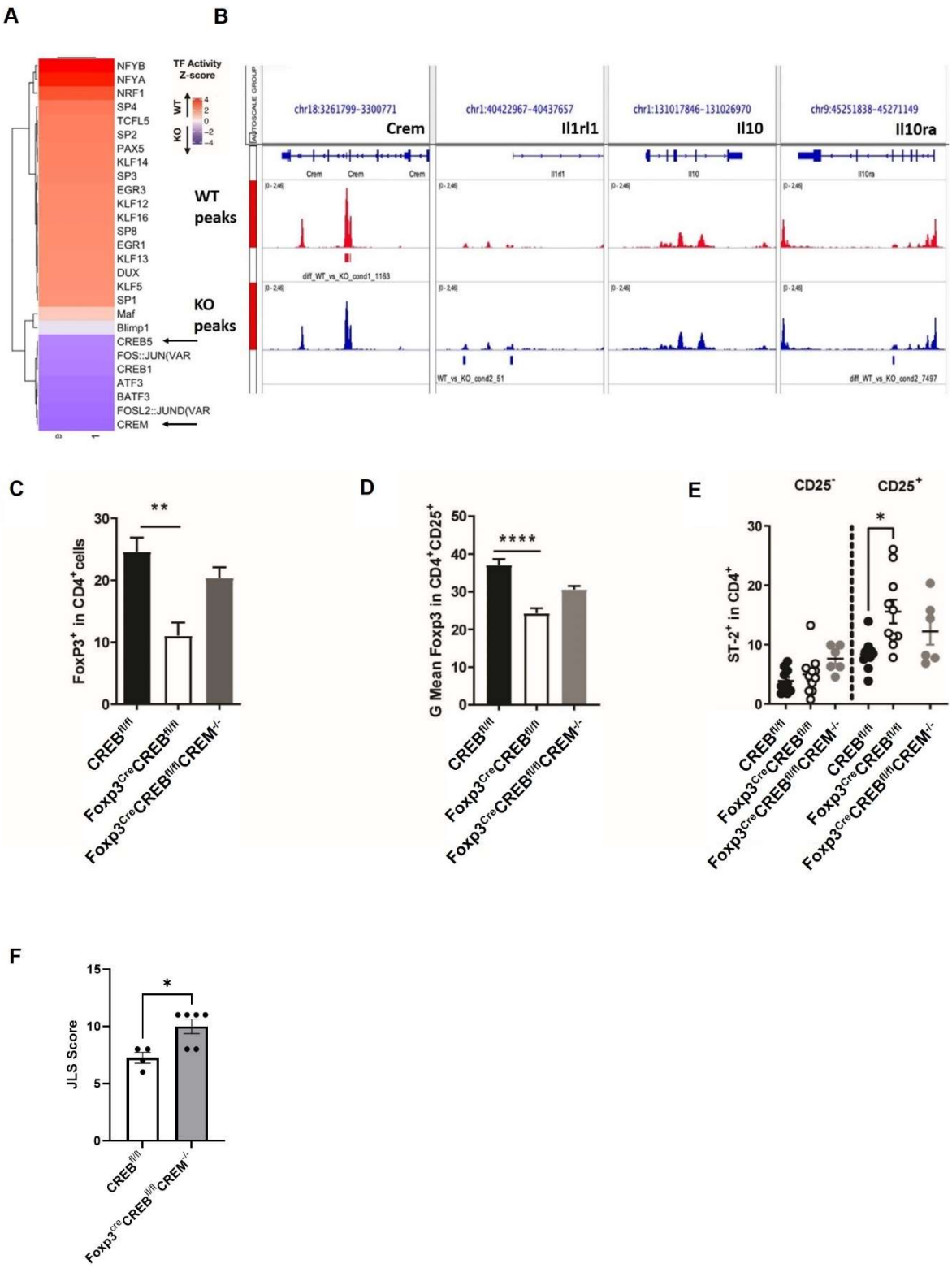

Figure 7: Genome-wide chromatin accessibility of *CREB*$^{fl/fl}$ and *Foxp3*^{cre}*CREB*$^{fl/fl}$ mice. A) ATAC-seq foot printing analysis indicates decrease in TF activity for CREB and CREM upon CREB KO and increase in TF activity of NRF1 upon CREB KO (p-value < 0.05; z-test). **B)** Example of genes with loss of chromatin accessibility upon CREB KO includes an alternative promoter of CREM (red peaks) and enhancer regions around SC-2/Il1nl1 (blue peaks) (adjusted p-value < 0.05; MACS2 diff. peak caller).

C) $CD4^+CD25^-$ T cells were stimulated with anti-CD3/CD28 antibodies in the presence/absence of 5 ng/ml TGF-β for five days. Percentages of $Foxp3^+$ cells from 6 independently performed experiments were determined, each with spleen from one mouse, *N* = 13 $CREB^{fl/fl}$, *N = 12* $Foxp3^{cre}CREB^{fl/fl,}$ and *N = 3* $Foxp3^{cre}CREB^{fl/fl}CREM^{-/-}$ mice, a two tailed unpaired t-test was used to test for significance, bars indicate mean and error bars SEM. **D)** Statistical analysis of MFI of Foxp3 in $CREB^{fl/fl}$ (*N* = 13) and $Foxp3^{cre}CREB^{fl/fl}$ (N = 9) and $Foxp3^{cre}CREB^{fl/fl}CREM^{-/-}$ (*N* =3) $CD4^+CD25^+$ T cells, bars indicate mean and error bars SEM, two tailed unpaired t-test was used to test for significance. **E)** Statistical analysis of $ST2^+$ in $CD4^+$ and $CD4^+CD25^+$ cells in $CREB^{fl/fl}$ (*N* = 5) and $Foxp3^{cre}CREB^{fl/fl}$ (*N = 6*) and $Foxp3^{cre}CREB^{fl/fl}CREM^{-/-}$ (*N* =3) $CD4^+CD25^+$ T cells, bars indicate mean and error bars SEM, one-way Anova test was used to test for significance. **F)** $Rag2^{-/-}$ mice were adoptively transferred with $CREB^{fl/fl}$ CD4 T-cells ($CD4^+$CD25-) or $Foxp3^{cre}CREB^{fl/fl}$ $CREM^{-/-}$ $CD4^+$ T cells (CD4+CD25-). Results of histological JLS (The Jackson Laboratory Scoring) score of colon sections (one experiment with overall *N=4/5* mice in each group, a two tailed Mann Whitney test was used to test for significance). *p<0.05, **p<0.01, ****p<0.0001 and results are expressed as the mean ± SEM.